0.875 in

8.5 x 10.875 in

A comprehensive system-level discussion of the geomicrobiology of the Earth's oceans

In *Systems Biogeochemistry of Major Marine Biomes*, a team of distinguished researchers delivers a systemic overview of biogeochemistry across a number of major physiographies of the global ocean: the waters and sediments overlying continental margins; the deep sub-surfaces; the Arctic and Antarctic oceans; and the physicochemical extremes such as the hypersaline and sulfidic marine zones, cold methane seeps and hydrothermal ecosystems.

The book explores state-of-the-art advances in marine geomicrobiology and investigates the drivers of biogeochemical processes. It highlights the imperatives of the unique, fringe, and cryptic processes while studying the geological manifestations and ecological feedbacks of *in situ* microbial metabolisms. Taking a holistic approach toward the understanding of marine biogeochemical provinces, this book emphasizes the centrality of culture-dependent and culture-independent (meta-omics-based) microbiological information within a systems biogeochemistry framework.

Perfect for researchers and scientists in the fields of geochemistry, geophysics, geomicrobiology, oceanography, and marine science, *Systems Biogeochemistry of Major Marine Biomes* will also earn a place in the libraries of policymakers and advanced graduate students seeking a one-stop reference on marine biogeochemistry.

Aninda Mazumdar is Principal Scientist of Geological Oceanography at CSIR-National Institute of Oceanography in Goa, India.

Wriddhiman Ghosh is Associate Professor in the Department of Microbiology at Bose Institute in Kolkata, India.

Cover Design: Wiley
Cover Image: © Wriddhiman Ghosh

www.wiley.com

WILEY

ISBN 978-1-119-55458-7

EDITED BY
MAZUMDAR
GHOSH

Systems Biogeochemistry of Major Marine Biomes

WILEY

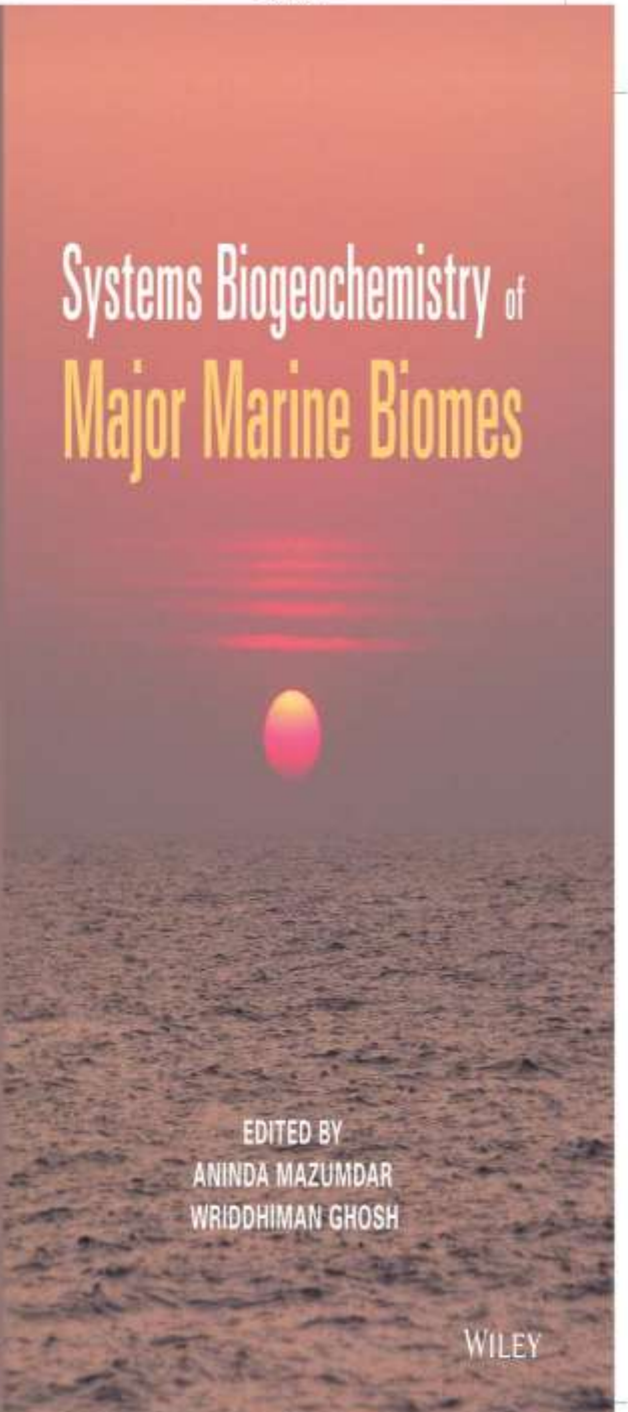

Systems Biogeochemistry of Major Marine Biomes

EDITED BY
ANINDA MAZUMDAR
WRIDDHIMAN GHOSH

WILEY

This edition first published 2022
© 2022 John Wiley & Sons, Inc.

All rights reserved. No part of this publication may be reproduced, stored in a retrieval system, or transmitted, in any form or by any means, electronic, mechanical, photocopying, recording or otherwise, except as permitted by law. Advice on how to obtain permission to reuse material from this title is available at http://www.wiley.com/go/permissions.

The right of Aninda Mazumdar and Wriddhiman Ghosh to be identified as the authors of the editorial material in this work has been asserted in accordance with law.

Registered Office
John Wiley & Sons, Inc., 111 River Street, Hoboken, NJ 07030, USA

Editorial Office
111 River Street, Hoboken, NJ 07030, USA

For details of our global editorial offices, customer services, and more information about Wiley products visit us at www.wiley.com.

Wiley also publishes its books in a variety of electronic formats and by print-on-demand. Some content that appears in standard print versions of this book may not be available in other formats.

Limit of Liability/Disclaimer of Warranty
In view of ongoing research, equipment modifications, changes in governmental regulations, and the constant flow of information relating to the use of experimental reagents, equipment, and devices, the reader is urged to review and evaluate the information provided in the package insert or instructions for each chemical, piece of equipment, reagent, or device for, among other things, any changes in the instructions or indication of usage and for added warnings and precautions. While the publisher and authors have used their best efforts in preparing this work, they make no representations or warranties with respect to the accuracy or completeness of the contents of this work and specifically disclaim all warranties, including without limitation any implied warranties of merchantability or fitness for a particular purpose. No warranty may be created or extended by sales representatives, written sales materials or promotional statements for this work. The fact that an organization, website, or product is referred to in this work as a citation and/or potential source of further information does not mean that the publisher and authors endorse the information or services the organization, website, or product may provide or recommendations it may make. This work is sold with the understanding that the publisher is not engaged in rendering professional services. The advice and strategies contained herein may not be suitable for your situation. You should consult with a specialist where appropriate. Further, readers should be aware that websites listed in this work may have changed or disappeared between when this work was written and when it is read. Neither the publisher nor authors shall be liable for any loss of profit or any other commercial damages, including but not limited to special, incidental, consequential, or other damages.

Library of Congress Cataloging-in-Publication Data

Names: Mazumdar, Aninda, editor | Ghosh, Wriddhiman, editor.
Title: Systems biogeochemistry of major marine biomes / edited by Aninda Mazumdar, CSIR-National Institute of Oceanography, Goa, India, Wriddhiman Ghosh, Bose Institute, Kolkata, India.
Description: First edition. | Hoboken, NJ : Wiley, 2022. | Includes bibliographical references and index.
Identifiers: LCCN 2021048467 (print) | LCCN 2021048468 (ebook) | ISBN 9781119554387 (cloth) | ISBN 9781119554370 (adobe pdf) | ISBN 9781119554363 (epub)
Subjects: LCSH: Biogeochemistry. | Chemical oceanography.
Classification: LCC QH343.7 .S97 2022 (print) | LCC QH343.7 (ebook) | DDC 577/.14–dc23/eng/20211103
LC record available at https://lccn.loc.gov/2021048467
LC ebook record available at https://lccn.loc.gov/2021048468

Cover image: © Wriddhiman Ghosh
Cover design by Wiley

Set in 10/12pt TimesNewRomanMTStd by Straive, Pondicherry, India

10 9 8 7 6 5 4 3 2 1

Copyrighted material

CONTENTS

Biome I Continental Margins

Biome II Ocean Depths

Biome III Polar Oceans

Biome IV Extreme Environments

14

Biogeochemical Characteristics of Hydrothermal Systems in the Indian Ocean

L. Surya Prakash[1,*], Sheryl Oliveira Fernandes[1,2], Baban Ingole[1], and John P. Kurian[1]

ABSTRACT

The Indian mid-oceanic ridge system is under explored for hydrothermal vent fields. Most vent fields are discovered along the slow to intermediate spreading Central Indian and ultra-slow spreading Southwest Indian ridges (CIR and SWIR). Detailed geological studies of Dodo, Solitaire, Edmond, Kairei, and Longqi vent fields and their fluids characteristics show that they are basalt-hosted systems. However, high hydrogen and methane concentrations in Kairei and Longqi fluids indicate fluid circulation through mafic–ultramafic lithologies. Abundant populations of (hyper)thermophilic hydrogenotrophic chemolithoautotrophs are associated with Dodo, Solitaire, and Kairei fluids. The Fe/Mn-oxidizing chemolithoautotrophs belonging to *Zetaproteobacteria* or various metal-tolerant genera within class Alphaproteobacteria and Gammaproteobacteria thrive on metal-rich Edmond and Longqui vent fluids. Therefore, the chemical composition of fluid and associated biosphere depend mainly on subsurface water–rock reactions and are independent of the spreading rate of the ridge. A very unusual animal community such as (i) vent crab *Austinograea rodriguezensis*, (ii) vent shrimps (*Rimicaris kairei*, and *Mirocaris indica*), (iii) deep-sea mussel (*Bathymodiolus marisindicus*), (iv) scaly-foot gastropods (*Chrysomallon squamiferum*, *Alviniconcha* sp.), and (v) barnacle (*Neolepas* sp.) are found at Indian Ocean vent fields. Most of the vent-specific fauna representing vent sites at the Central and Southwest Indian Ridges are found at Kairei field (> 24% of the total), making it biologically diverse and supporting the hypothesis that the Rodriguez Triple Junction (RTJ) could be an essential connecting point for dispersal of larvae to the nearby vent fields. Further, the Southwest–Southeast Indian Ridges could act as a corridor for dispersal of vent fauna between Atlantic, Indian and Pacific Oceans. Interestingly, similar chemosynthetic vent fauna (associated with Galatheidae, Neolepadidae, and Mitilidae families) have also been found at cold-seep methane hydrate systems in Indian continental margins. Detailed genomic studies of cold-seep community and its comparison with vent community and water column hydrothermal tracer-based studies are required to establish the ecosystem connectivity.

14.1. INTRODUCTION

14.1.1. Hydrothermal Circulation: Evolution of Fluids and Associated Chemosynthetic Ecosystem

Hydrothermal circulation plays a vital role in the cycling of elements, energy, and mass between the solid Earth and the Ocean (Lang, 2018; Urabe et al., 2015). It mainly

---

[1] *ESSO-National Centre for Polar and Ocean Research, Ministry of Earth Sciences, Headland Sada, Vasco-da-Gama, Goa, 403804, India*

[2] *Present address: School of Earth, Ocean and Atmospheric Sciences, Goa University, Taleigao Plateau Goa, 403206, India*

**Corresponding Author: Surya Prakash (surya@ncpor.res.in) ORCiD code: 0000-0003-0830-2145*

Systems Biogeochemistry of Major Marine Biomes, First Edition. Edited by Aninda Mazumdar and Wriddhiman Ghosh.

occurs at the fractured volcanic mid-ocean ridge system that extends over ~ 6 × 10^4 km, in which cold seawater percolates down through cracks in the oceanic crust and becomes heated (German and Von Damm, 2003). The chemical composition of seawater is modified during its reaction with the subsurface host rock. The modified seawater becomes hot and extraordinarily buoyant and rises back to the seafloor. These expelled vent fluids have high enrichments of dissolved gases, such as helium (^3He), hydrogen (H_2), methane (CH_4), carbon dioxide (CO_2), trace metals (e.g., Fe, Mn, Cu, Ni, Zn, Pb), and depletions such as Mg and SO_4 compared with ambient seawater. Most of the dissolved chemicals in hydrothermal fluids precipitate as (i) polymetallic-sulfides within cracks of host rocks as vein deposits, as mounds, and as thick columns named chimneys, and (ii) polymetallic oxyhydroxides and silicates upon mixing with the cold seawater (2 °C).

The chemical compositions of the fluids provide information on the depth of fluid circulation, heat source, pressure, and temperature (PT) conditions of the reactions they have experienced during their transit (residence time of fluids) through the crust. Generally, it is well understood that the percolated seawater is modified by the varying PT conditions, water–rock interactions, and various biological processes within the crust. Water–rock interaction processes begin during the downflow leg of seawater in the recharge zone, and they are indistinguishably connected (Figure 14.1). During fluid circulation, the seawater is modified and evolves as hydrothermal fluids, which are reducing because of the presence of H_2S. It is acidic and gains many metals (e.g. Fe^{2+} and Mn^{2+}) and gases (e.g. H_2, CO_2, CH_4, and ^3He) and trace elements (e.g. cobalt, nickel, copper, zinc, aluminum, silver, barium, tungsten, gold, lead, and rare earth elements, REE) by leaching them out from the rocks.

Chemical compounds spewed out through vent fluids support various chemolithoautotrophic microorganisms, which form the base of the food web for numerous animals associated with deep-sea hydrothermal ecosystems. The chemical composition of vent fluids can be altered by chemolithoautotrophic microbes during subsurface circulation. However, the biological influence on overall chemical fluxes, how widespread they are, and which elements are affected remain to be resolved. Recent studies (TAIGA concept: Trans-crustal Advection and *In-situ* biogeochemical processes of Global sub-seafloor Aquifers) have shed some light on the role of biology in sub-seafloor hydrothermal circulation (Urabe et al., 2015).

The buoyant high-temperature fluids expelled to the cold stratified oceanic water column from the vent lead to the formation of hydrothermal plumes (Figure 14.2). They are important for heat and energy as they can act as a driving force for mid-depth oceanic circulation (Helfrich and Speer, 1995), gross chemical fluxes (German et al., 1991), and for transporting both chemical compounds and larvae of many faunal species from one adjacent vent site to another (Van Dover et al., 2002). As the hydrothermal plume rises in the water column, it becomes progressively less buoyant and produces turbulence and eddies, which entrains seawater. In this process, the original vent fluid gets diluted, and it cannot rise beyond a finite maximum height of approximately 300–400 m above the seafloor (Figure 14.2). At this stage, the diluted hydrothermal fluid begins to disperse laterally, which is known as a non-buoyant plume or neutrally buoyant plume, and represents both directions of gene flow along the global mid-oceanic ridges and biogeochemical processes within. Potential sources of microorganisms in hydrothermal plumes primarily include communities from ambient seawater, vent chimneys, near-vent animal

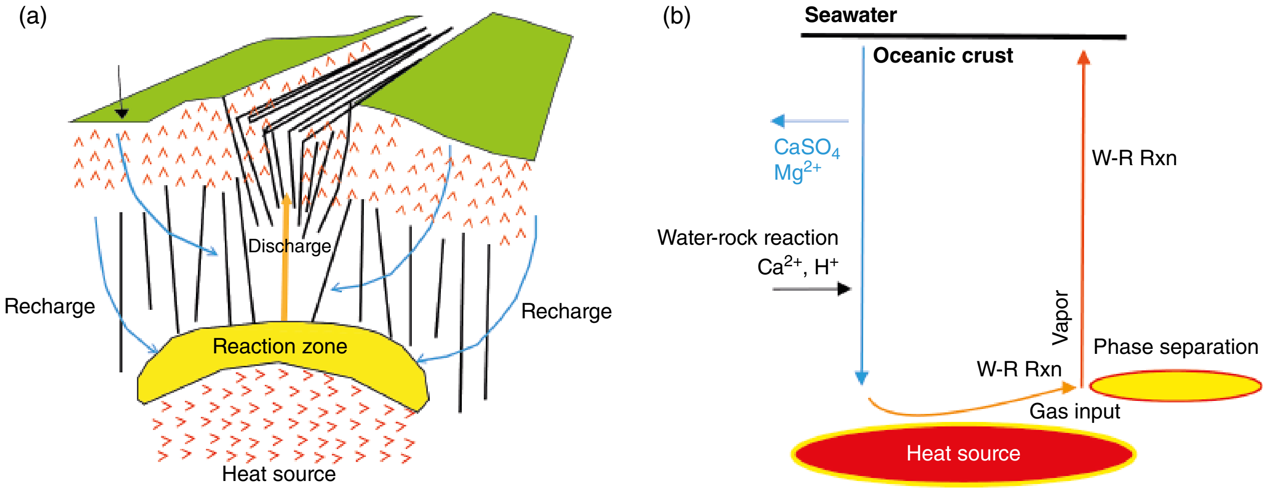

Figure 14.1 (a) Schematic illustration of three stages: recharge, reaction, and discharge of hydrothermal circulation (modified after German and Von Damm, 2003). (b) Schematic diagram shows the processes that control the chemical composition of hydrothermal vent fluid (after German and Von Damm, 2003). W-R RXN, water–rock reaction.

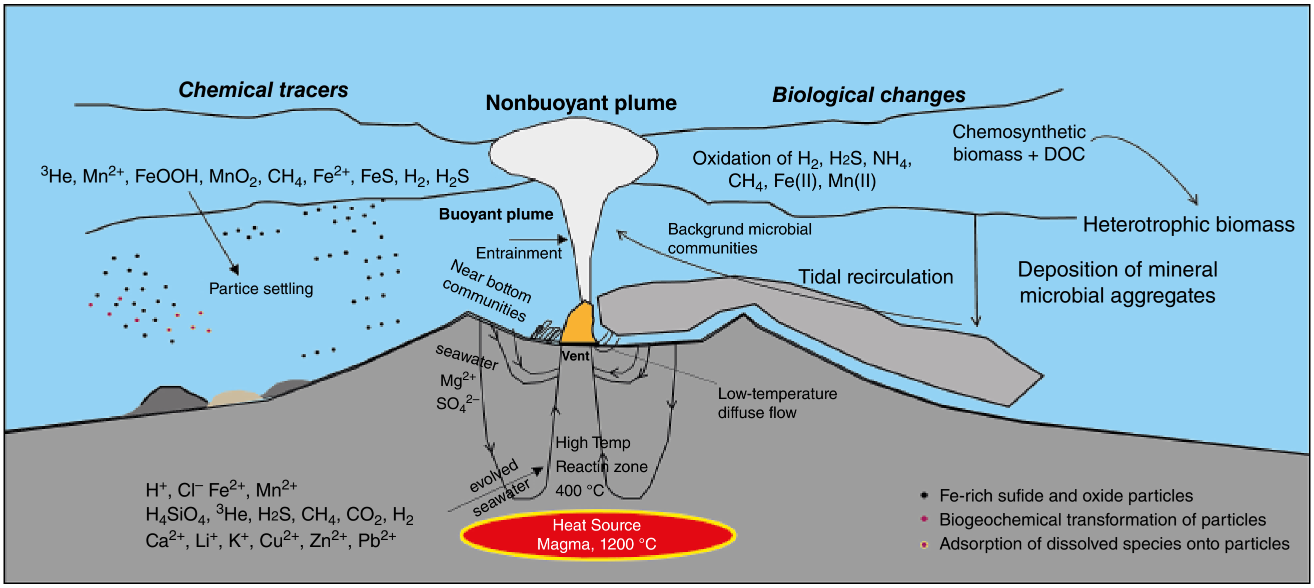

Figure 14.2 Schematic illustration of a hydrothermal plume in the deep water depicting dispersal of vent-derived chemical compounds, sources of plume microorganisms, and changes caused by them to hydrothermal components in ambient seawater. DOC, dissoved oranic carbon.

symbioses, subsurface environment, near-bottom waters, recirculation of aged plume or those growing within the plume (Figure 14.2; Dick et al., 2013). Nevertheless, plume chemical composition and microbes are distinct from those in the ambient water column (Winn et al., 1986; Naganuma et al., 1989; Juniper et al., 1998; Maruyama et al., 1998; German and Von Damm, 2003; Lam et al., 2004, 2008; Dick et al., 2009).

The vent fauna consumes the chemolithoautotrophic microbial mats that grow at hydrothermal vents. This is quite a contrast to the fauna associated with abyssal and seamounts sustained by the supply of phytodetritus from the water column (Van Dover 2000). Moreover, most of the chemosynthetic habitats occur discretely at geographically isolated sites. Therefore, the fauna associated with these ecosystems has unique survival strategies regarding reproduction and larval dispersal (Mullineaux et al., 2018). Alhough the Indian Ocean is considered the most biologically diverse, it is also under-sampled and ecologically less studied.

The diversity of vent specific communities has been described by many researchers (Haymon et al., 1993; Hashimoto et al., 2001; Van Dover et al., 2001; Nakamura et al., 2012; Beedessee et al., 2013; Chen et al., 2015; Copley et al., 2016; Watanabe et al., 2018; Zhou et al., 2018; Jang et al., 2020; Sun et al., 2020). However, most of the known hydrothermal vents sites are located in the Pacific and Atlantic Oceans, and very few active vent fields have been discovered in the Indian Ocean (Gamo et al., 2001; Hashimoto et al., 2001; Van Dover et al., 2001; Tao et al., 2011, 2012, 2014; Nakamura et al., 2012, 2013; Copley et al., 2016; Ji et al., 2017). Studies on the biodiversity and biogeography of Indian Ocean vent fauna were initiated only after discovering the Kairei vent field (Van Dover et al., 2001). Although the hydrothermal vents along the CIR and SWIR are located within a limited area, they are considered reasonably diverse in terms of biological communities associated with them (Nakamura and Takai, 2015b).

A chemosynthetic ecosystem similar to hydrothermal vents was also discovered recently on the eastern continental margins of India (Mazumdar et al., 2019). In 2009, chemosynthetic clams shells (*Calyptogena* sp.) associated with carbonates (methane derived) were reported in sediment cores collected from the Krishna–Godavari basin as evidence for paleo-cold seep activity (Mazumdar et al., 2009). Ten years later, in 2019, a shallow methane hydrate zone associated with the cold-seep ecosystem (chemosymbiont bivalves, polychaetes, and gastropods) was reported by Mazumdar et al. (2019). Bivalves comprised five genera from family *Provannidae* and family *Neritidae* represented by *Bathymodilus*, *Calyptogen Canchocele*, *Acharar* and *Pectin*, and Gastropoda. Polychaeta (Phylum: Annelida) was the second most dominant and was represented by four species (*Branchipolynoe seepensis*, *Sclerolinum* sp., *Glycera* sp., and *Serpulidae* sp.). The cold-seep system has similarities to the typical hydrothermal vent system at mid-oceanic ridges in which the ecosystem survives on chemical species such as H_2, H_2S, CH_4, Fe (II) (Fisher et al., 2007; Levin and Sibuet, 2012; Takai and Nakamura, 2010). The main difference is the temperature. The ecosystem at hydrothermal vents is surviving at a relatively higher temperature than the cold-seep methane system. Both hydrothermal vents and cold seeps provide energy for the most unusual ecosystems on Earth (Le Bris et al., 2016). Many species of cold seeps with numerous families and genera are shared with hydrothermal vents (Bernardino et al., 2012). Evidence for both types of ecosystems is available at Mariana Arc or Costa Rica margin (Watanabe et al., 2010).

In the Indian Ocean, the CIR and SWIR have been relatively more explored to ascertain vent/plume chemical components and associated microbial communities and hence will be dealt with in detail. Microbial diversity associated with actively venting sites is strongly connected to chemical gradients of hydrothermal fluids. However, microbial investigations of vent specific-fauna of hydrothermal systems in the Indian Ocean region are far fewer and they remain poorly explored. In this chapter, an attempt has been made to understand: (i) the geochemical composition of hydrothermal fluids in relation to source rock; (ii) to establish a link between geochemical composition and microbial abundance/community distribution patterns in various vent fields in the Indian Ocean; and (iii) vent fauna associated with hydrothermal vents along the Indian mid-oceanic ridges and its connection with fauna associated with cold-seep methane hydrate system.

14.2. GEOLOGICAL AND OCEANOGRAPHIC SETTINGS OF THE INDIAN OCEAN

The Indian Ocean is the third biggest among world oceans and covers approximately 20% of the water on the Earth's surface. Compared with other oceans, the Indian Ocean is the youngest, most physically complex, and constitutes four active spreading ridges, namely the Carlsberg Ridge (CR), CIR, SWIR, and the Southeast Indian Ridge (SEIR), which are parts of the world mid-ocean ridge system (Figure 14.3). Along with these, the longest aseismic ridges (Chagos–Laccadive, Ninety East Ridge,

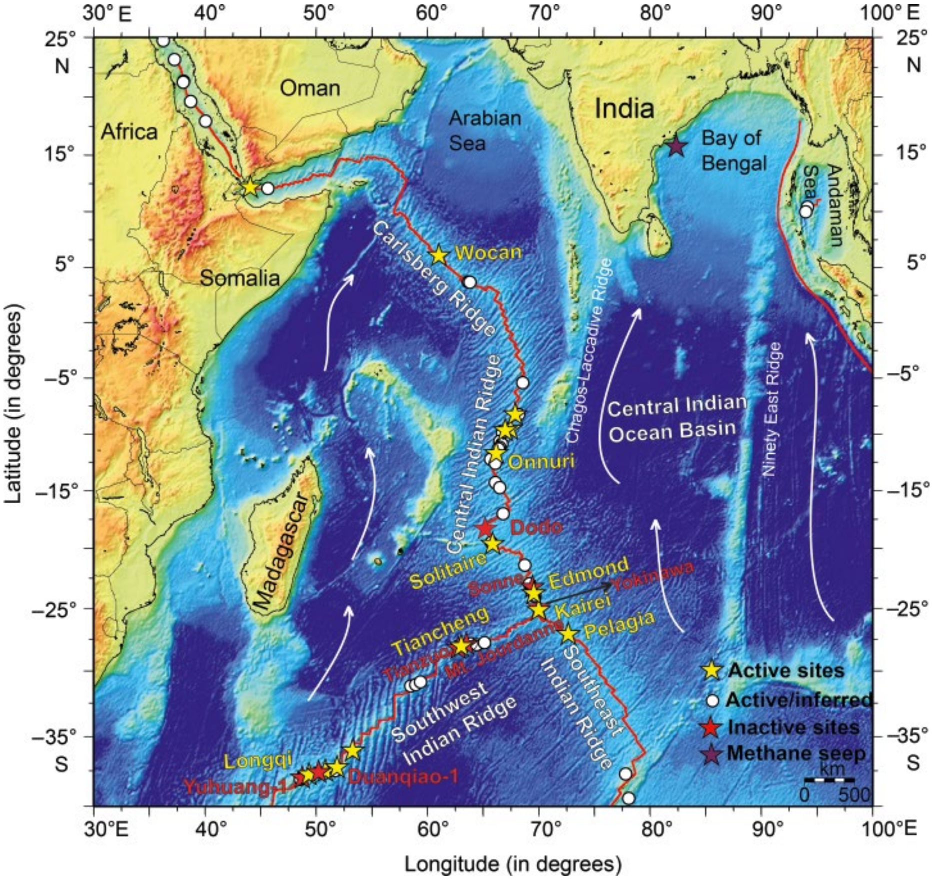

Figure 14.3 Geological setting of the Indian Ocean, which includes mid-oceanic ridges (Carlsberg Ridge, Central Indian Ridge, Southwest Indian Ridge, and Southeast Indian Ridge), aseismic ridges (Chagos–Laccadive and Ninety East ridge), and convergent plate boundary (Andaman back-arc basin). Active and inactive hydrothermal vent fields along the Indian mid-oceanic ridges are named and represented as yellow and blue stars. Active hydrothermal vents (unconfirmed) and plumes are shown as white circles. The cold seep methane hydrate zone is represented by a red star. The white line represents the general deep and bottom water flow in the Indian Ocean (redrawn from Mantyla and Reid, 1995; Piotrowski et al., 2009; Wilson et al., 2012).

Comorin Ridge, and Broken Ridge) and abyssal basins (Central Indian Ocean Basin, CIOB, Somali, Mascarene, Madagascar, and Mozambique basins); several plateaus (Agulhas, Kerguelen, Mascarene, Naturaliste, Wallaby, and Zenith) and seamounts are major structural features of the Indian Ocean.

The CR in the northwest Indian Ocean defines the plate boundary between the Indian and Somalia plates. The CR begins at the Owen fracture zone near 10°N and extends to the CIR near the equator with a northwest–southeast trend (Figure 14.3). The CR is a typical slow-spreading ridge with an average half-spreading rate of 11 to 16 mm/yr, a V-shaped rift valley, and a wide valley floor (Kamesh Raju et al., 2008). The Carlsberg Ridge is also characterized by rugged topography like the CIR, steep valley walls, and wide rift valley floor (13–26 km), which are characteristics of a slow-spreading ridge. Along the ridge axis mantle-derived peridotite was recovered from the inner valley floor (Ray et al., 2012), suggesting distinct variations in accretionary processes along the ridge.

The CIR, north of the Rodriguez Triple Junction (RTJ), is also a slow to intermediate spreading mid-ocean ridge in the Indian Ocean. The segmentation pattern of the 750 km long CIR between 3°S and 11°S (Figure 14.3) has been studied using multibeam bathymetry and magnetic data (Kamesh Raju et al., 2012b). The ridge has well-defined spreading segments and a wide rift valley floor 12–15 km wide, steep valley walls, rugged topography, and prominent volcanic constructional ridges on either side of the central rift valley (Kamesh Raju et al., 1997). These characteristics define the CIR to be a slow-spreading ridge. The spreading rates are slightly higher (average full spreading rates varying from 26 to 38 mm year^{-1}) than the slow-spreading CR. In the southern part of the CIR, the spreading rate is 47 mm year^{-1} (DeMets et al., 2010). Both the SWIR and SEIR meet the CIR at 25°S and form a ridge–ridge–ridge triple junction named the Rodriguez Triple Junction.

The SWIR extends from the RTJ at 25°S to the Bouvet Triple Junction (BTJ) at 0°E; 55°S, which is ~8000 km in length. With a full spreading rate of 14 mm year^{-1}, the SWIR is classified as an ultra-slow spreading ridge (Patriat and Segoufin, 1988; DeMets et al., 1994; Cannat et al., 2008). Absence of volcanic activity, insufficient melt supply, smooth topography, deep axial valley, and exposure of mantle-derived rocks in the axial valley and at some places with gabbro and basaltic rocks are characteristics of SWIR (Royer et al., 1988; Mendel et al., 1997; Mendel and Sauter, 1997; Sauter et al., 2001; Dick et al., 2003; Cannat et al., 2006, 2008). The SEIR extends from the RTJ at 25°S to the Macquarie Triple Junction (MTJ) at 162.76°E; 63°S and is approximately 6000 km long (Cochran and Sempéré, 1997). The SEIR is classified as an intermediate spreading ridge with a full spreading rate of 59–75 mm year^{-1} (Royer and Sandwell, 1989; Cochran and Sempéré, 1997; Small et al., 1999; DeMets et al., 2010).

The deep Indian Ocean is only ventilated from the south and flushes with the Antarctic Bottom Water (AABW) which is carried by the Antarctic Circum-polar Current (ACC), and North Atlantic Deep Water (NADW) carried by the Deep Western Boundary Current (DWBC) flow northward (Piotrowski et al., 2009). The Antarctic waters flow through Enderby Basin, on the west, and through Australian–Antarctic Basin (AAB), on the East (Vlastélic et al., 2001). The origin of water in the Enderby basin is mainly from the Weddell Sea, which flows through a gap in the SWIR and a gap between the Crozet and Kerguelen Plateaus. The same water spreads into the basin on the western side through the Crozet, Madagascar, Mascarene, and Somali basins and finally reaches the Arabian Sea. In contrast, water in the AAB originates from the Ross Sea, enters via the SEIR and spreads northwards into the Central Indian Basin. The general flow of bottom waters, such as AABW and NADW, in the western Indian Ocean, follows a south to north trend (Kumar and Li, 1996; Wilson et al., 2012).

14.3. HYDROTHERMAL VENT FIELDS IN THE INDIAN OCEAN

14.3.1. Chemical and Microbiological Aspects of Vent Fluids and Plume Waters

Indian Ocean ridges are poorly explored for hydrothermal vents when compared with the global mid-oceanic ridge system. Among the vent fields discovered, detailed studies on vent fluid chemical and microbiological characteristics in combination with geological setting are available for only five fields: Dodo, Solitaire, Edmond, and Solitaire along the CIR, and Longqi in the SWIR. Therefore, our discussion in this section will be focused mainly on these five fields.

Dodo

The Dodo field (18°20.1′S, 65°17.9′E; water depth of 2745 m) is located on the Dodo great lava plain where morphological characteristics of high-production basaltic melt are reported (Okino et al., 2015). It is similar to fast-spreading ridges such as the East Pacific Rise (EPR). Hydrothermal fluids from this field have high temperatures (356 °C) while the pH is 3.2. They are enriched in hydrogen (>2 nM) and chlorine (20%) compared with seawater (Table 14.1) and indicates sub-seafloor circulation through serpentinization of rocks and phase-separation (Kawagucci et al., 2008). However, the morphological features of these segments show only large-scale basaltic sheet-flow lava in this region

Table 14.1 Hydrothermal vent fluid compositions for different vent fields and seawater in the Indian Ocean.

Vent Field	Dodo	Solitaire	Edmond	Kairei	Longqi	Seawater
Location	18°20.1′S, 65°17.9′E	19°33.41′ S, 65°50.88′ E	23°52.68′S, 69°35.80′E	25°19.23′S, 70°02.42′E	49°39′E, 37°47′S	
Host Rock	Fresh Basalt (E-MORB)	Basalt (E-MORB)	Basalt (N-MORB)	Troctolite + D-MORB	Basalt	
Depth(m)	2745	2606	3270–3303	2420–2452	2765	
Temperature (°C)	356	307	382	359	365–379	2
pH (25°C)	3.27	4.40	3.13	3.36–3.50	3.58–3.68	7.8
Cl (mM)	684	489	927–950	637–642	612–614	542
Na (mM)	566	409	717–721	534–560	492–496	465
H_2 (mM)	2.70	0.43	0.12–0.14	2.97–3.89	0.16–0.20	<0.01
CH_4 (mM)	0.025	0.043	0.22–0.31	0.10–0.20	0.36–0.38	<0.01
CO_2 (mM)	4.6	16.2	5–13.7	3.94–10.1	–	–
H_2S (mM)	2.80	4.75	4.81	4.00	–	0
$^{3/4}$He (R_{atm})	7.18	8.96	–	7.8	–	1.13
Mn (μM)	917	78	1430	840	1271–1392	<0.001
Fe (μM)	5408	60	13900	5400	10950–11660	<0.001

Data are compiled from: Van Dover et al. (2001), Gallant and Von Damm (2006). Kumagai et al. (2008), Nakamura et al. (2012), and Kawagucci et al. (2016) for CIR; and Ding et al. (2017), Ji et al. (2017), and Yue et al. (2019) for SWIR.
MORB, mid-ocean ridge basalt; D-MORB, depleted.; E-MORB, enriched; N-MORB, normal.

(Okino et al., 2015), and ultramafic rocks are found over the Marie Celeste Fracture Zone (Hekinian, 1982), which is 50 km away from the vent field. Hence, it could be inferred that the hydrogen enrichment might have resulted from magmatic events and subsequent incipient fluid–rock interaction. An end-member concentration of Fe (5408 μM) and Mn (917 μM) indicates rapid sub-seafloor fluid cooling owing to a relatively shallow heat source and insufficient fluid–rock interaction (Kawagucci et al., 2016).

Hydrothermal fluid discharges and animal colonization at the Dodo field has ceased in the recent past (Kawagucci et al., 2016). The microbial cell density in the chimney (Tsukushi-1, Tsukushi-2, and Potsunen) habitats of the Dodo vent field have been reported to be similar in magnitude (10^7 cells g^{-1}; Kawagucci et al., 2016) to those from the Kairei hydrothermal field (KHF) (Takai et al., 2004a). Moreover, high H_2 concentrations in vent fluids, as in the KHF, support abundant populations of (hyper)thermophilic hydrogenotrophic chemolithoautotrophs such as methanogens and hydrogen- and sulfur-oxidizing bacteria that were closely related to the genera *Methanopyrus*, *Methanocaldococcus*, *Persephonella*, and *Sulfurimonas* (Kawagucci et al., 2016).

Solitaire

The Solitaire hydrothermal field lies within the Exclusive Economic Zone (EEZ) of the Republic of Mauritius and is located (19°33.413′S, 65° 50.888′E, at a water depth of 2606 m) several kilometers away from the ridge axis on the western flank of the CIR (Nakamura et al., 2012). The basalt-hosted field is ~50 × 50 m and has three major chimney sites – Toukon-3 (black smoker), Tenkoji, and Liger chimney (both with clear fluids) which are < 5 m high, with small mounds at their feet (Nakamura and Takai, 2015a). The hydrothermal fluids have a high temperature (307 °C) and are depleted in chlorine (10%) compared with seawater. This indicates phase-separation and segregation of a vapor-rich phase in discharging fluids (Nakamura et al., 2012; Nakamura and Takai, 2015b; Kawagucci et al., 2016). However, the hydrogen concentration of 0.46 mM (Nakamura and Takai, 2015b) is relatively low and comparable with typical hydrothermal fluids from mid-oceanic ridges (MOR (McCollom 2008). A relatively high pH of 4.8 (Table 14.1) indicates subseafloor mixing of hydrothermal fluids and seawater. The relatively low concentrations of Fe and Mn (60–78 μM) compared with other hydrothermal fluids of Dodo, Edmond, Kairei, and Longqi, indicates that subseafloor fluid cooling has been sufficiently long for fluid–mineral interaction (Kawagucci et al., 2016). The gas chemistry of hydrothermal fluids (CO_2, H_2 and CH_4), is comparable to the typical mid-oceanic ridge basalt-hosted system (Table 14.1). A high helium concentration ($R_S/R_{atm} = 8.96$; where R is the ratio of $^3He/^4He$ in sample and atmosphere) indicates the hotspot influence on the fluid chemistry, which is further supported by helium-rich basalts from this region (Füri et al., 2011). The Solitaire field is characterized by multiple diffuse flows from the talus throughout the hydrothermal field (Nakamura et al., 2012).

Permeable mineral structures and continued mixing of chemically reduced fluids and oxidized seawater provide favorable conditions that support the growth of endolithic microbial communities (Schrenk et al., 2003). Microbial cell density in the exterior surface of the Toukon-3 chimney fragment has revealed 2.1 × 10^4 cells g^{-1} whereas the inside part of the chimney harbored 2.4 × 10^3 cells g^{-1} (Kawagucci et al., 2016). Quantitative polymerase chain reaction (PCR) analysis of the 16S rRNA gene also revealed the highest bacterial abundance (10^5 copies g^{-1}) in the exterior surface of the Toukon-3 chimney but no detectable archaeal gene copy numbers. Members of Aquificales and Epsilonproteobacteria dominated the microbial community on the surface of the Toukon-3 chimney. Vent endemic Epsilonproteobacteria are responsible for actively oxidizing sulfur (Akerman et al., 2013). The Aquificales, with a microaerophilic and thermophilic bacterial lineage, and capable of oxidizing hydrogen, have been reported from deep-sea vents in the Mid-Atlantic (Reysenbach et al., 2000) and Indian Oceans (Reysenbach et al., 2002). Quantitative cultivation-based test revealed the existence of (hyper)thermophilic, hydrogenotrophic chemolithoautotrophs at the Toukon-3 chimney, which were most closely related to genera *Persephonella* and *Sulfurimonas*. Members of the genus *Persephonella* appear to be key players in carbon, sulfur, and nitrogen cycles in high-temperature habitats such as deep-sea vents (Mino et al., 2013). *Sulfurimonas* species have been isolated from sulfidic habitats (Inagaki et al., 2003) and can grow with nitrate or nitrite as electron acceptors and with a variety of sulfur species of different oxidation states or use hydrogen as electron donor (Labrenz et al., 2013). Genetic variation of 109 *Sulfurimonas* strains isolated from four geographically distant deep-sea hydrothermal vent regions (Okinawa trough, Mariana volcanic arc and trough, Central Indian Ridge, and the Mid-Atlantic Ridge) have also been studied based on 11 protein-coding genes. These included strains from the Solitaire vent field. High genetic variation corresponding to hydrothermal regions was observed, which indicated that allopatric speciation in the *Sulfurimonas* population was primarily influenced by geographical distance rather than the gas composition of vent fluid or habitat (Mino et al., 2017).

Edmond

The Edmond hydrothermal field is located (23°52.68′S, 69°35.80′E; water depth of 3290–3320 m) in an off-axis region of the northern end of the ridge segment (Van Dover et al., 2001) where typical abyssal hills are observed (Kumagai et al., 2008). The main area of hydrothermal venting in the Edmond hydrothermal field is spread to ~ 100 × 60 m, with black smoker complexes of up to 35 m high and 2 m diameter (Gallant and Von Damm, 2006). The most vigorous black-smoker venting is located in discrete clusters of large chimneys at the Nura Nura vent site (Kumagai et al., 2008). The field is dominated by old, disaggregated sulfide structures and massive sulfide taluses, which are suggestive of focused hydrothermal activity over several years (Van Dover et al., 2001). The fluid temperature of 382 °C (Table 14.1) is the highest ever measured in the Indian Ocean, with a pH range from 2.97 to 3.30 (Gallant and Von Damm, 2006; Kumagai et al., 2008). Chlorine concentrations are quite high (> 70%) when compared with seawater, indicating subseafloor phase separation along with brine condensation. However, hydrogen concentrations are relatively low and are comparable with fluids from EPR and Mid-Atlantic Ridge (MAR). Like the Solitaire hydrothermal field, extensive diffuse flows have been reported from the Edmond field (Nakamura and Takai, 2015a).

Orange-brown, iron oxyhydroxide sediments several centimeters thick have been found to accumulate in depressions, coating many sulfide structures and taluses in the Edmond field (Van Dover et al., 2001). Extensive microbial mats have also been found to cover the surface of sediments, which have been attributed to widespread sub-surface seawater entrainment and mixing processes (Van Dover et al., 2001). Rod-shaped microbes with s helical stalk-like filaments have been observed in microbial mats from a hollow inside a chimney structure from the Edmond field (Peng et al., 2007). *Mariprofundus ferrooxydans*, a neutrophilic, mesophilic, and iron-oxidizing chemolithoautotrophic marine bacterium affiliated to class *Zetaproteobacteria*, and isolated from iron-rich mats in hydrothermal fields of the Loihi Seamount (Emerson et al., 2007) has been shown to produce unique helical stalks consisting of organic compounds and iron oxides (Chan et al., 2011). It is likely that *Zetaproteobacteria* could also be dominating iron-rich mats (Kato et al., 2009) in the Edmond field. Bioprecipitation of Fe on the surface and in the interior of cells has been observed to occur along with microbial silicification in the mats (Peng et al., 2007). Scanning electron micrographs of mineralized crust samples have revealed abundant filamentous rod, and coccoidal forms encased in sulfur and sulfide mineral precipitates. These observations suggest that the biomineralization process by thermophilic chemolithoautorophs might be dependent on hydrothermal inputs (Peng et al., 2007) and may influence the architecture and sulfur cycling of sulfide spires in the vent field (Hoek et al., 2003).

Phylogenetic analysis of microbial communities associated with the mineralized crust coating a sulfide spire collected from the Edmond vent field revealed 26 bacterial and nine archaeal phylotypes (Hoek et al., 2003). More than 90% of the bacterial phylotypes were primarily affiliated with Epsilonproteobacteria. In contrast, the majority (97%) of the archaeal phylotypes grouped with the Deep-sea Hydrothermal Vent Euryarchaeotal Group (DHVEG) that appears to be endemic to vent ecosystems. The sulfur oxidation *soxB* gene of Epsilonproteobacteria from diffuse hydrothermal fluids suggests that *Sulfurimonas*-like species are responsible for actively oxidizing sulfur via the Sox pathway (Akerman et al., 2013). These autotrophic and mixotrophic sulfur-oxidizing bacteria (Sievert et al., 2008) can also use other electron acceptors such as nitrate, nitrite, and fumarate (Vetriani et al., 2004; Miller et al., 2007) and fix carbon via the reductive tricarboxylic acid (rTCA) cycle (Hügler et al., 2005). Archaea affiliated to DHVEG have been suggested to be obligate thermoacidophilic sulfur- or iron- reducing heterotrophs (Reysenbach et al., 2006). The thermophilic hydrogen-oxidizing *Hydrogenobacter thermolithotrophum* and hyperthermophilic sulfur-reducing *Thermococcales* have also been reported from sulfide spires from the Edmond vent field (Hoek et al., 2003).

Two primary lineages of Aquificales, *Persephonella marina* (Type strain HI) and *Persephonella* sp. nov. strain H3, were cultured in an enriched medium that was inoculated with ground sulfide samples obtained from the Edmond vent field (Reysenbach et al., 2002). These thermophilic, strictly chemolithoautotrophic, hydrogen-oxidizing microaerophiles have been reported from deep-sea hydrothermal vent sites in the Pacific Ocean (Takai et al., 2008; Mino et al., 2013). These bacteria grow at a temperature range between 55 and 80 °C and pH 4.7–7.5. They can use elemental sulfur, thiosulfate, or hydrogen as electron donors, while oxygen/nitrate is used as electron acceptors (Götz et al., 2002). Their occurrence at deep-sea vents globally has expanded our knowledge on their distribution. This knowledge reflects their preference to thrive in high-temperature, acidic fluids like those from the Edmond vent field.

Kairei

The Kairei hydrothermal field (KHF) is located (25°19.23′S, 70°02.42′E; water depth of 2415–2460 m) near the RTJ. Here, several hydrothermally active sites had been suggested to exist around the off-axis Hakuho knoll, which is ~ 6.4 km northeastward from the ridge axis of the CIR (Gamo et al., 1996). Several black smoker complexes with a maximum height of >10 m have been recognized in the 40 × 80 m field (Gamo et al., 2001), along with large areas of weathered sulfides and inactive chimneys (Nakamura and Takai, 2015a). The most vigorous black smoker discharges have been observed at the Kali vent site (Kumagai et al., 2008). The hydrothermal fluid temperature of 369 °C and pH range of 3.3–3.6 of the Kairei vent field are comparable with the Edmond field (Table 14.1). The chlorine concentrations are slightly higher (14%) compared with those of normal seawater. Based on basalt rocks and the chemical composition of fluids, the field was initially assumed to be a typical basalt-hosted hydrothermal system. Later studies have revealed enrichment of hydrogen (2.5–8.5 mM; Gamo et al., 2001; Van Dover et al., 2001; Gallant and Von Damm, 2006) and well-defined oceanic core complex structure with peridotite and gabbros. The field may have developed by seawater circulation through subsurface ultramafic rocks similar to hydrothermal fields along MAR (e.g. the Rainbow, Logatchev I and II, Ashaze I and II, and Nibelungen).

A microbial density of up to 2.3×10^6 cells l^{-1} has been detected in superheated Kali vent fluids (Takai et al., 2004). In the Fugen chimney vent orifice, which is ~ 50 m away from the Kali chimney (Takai et al., 2004), up to 10^7 cells g^{-1} wet weight were found. These values are much higher than those reported from high-temperature chimney fragments from the Solitaire hydrothermal fluids (Kawagucci et al., 2016). Takai et al. (2004) proposed that the Kairei ecosystem is sustained through primary production by hydrogenotrophic, hyperthermophilic methanogens, which utilize H_2 and CO_2 as primary energy and carbon sources. The thermophilic, methanogenic autotrophs *Methanocaldococcus indicus* (L'Haridon et al., 2003), *Thermodesulfatator indicus* (Moussard et al., 2004), *Methanotorris formicicus* and *Hydrogenimonas thermophila* (Takai et al., 2004) isolated from KHF were capable of using H_2 and CO_2 as sole energy and carbon sources. Subsequent studies using *Methanopyrus kandleri* strain 116, a dominant hyperthermophilic methanogen isolated from an *in situ* colonization system deployed in black smoker fluid of the KHF, were conducted under high temperatures (85–123 °C) and hydrostatic pressures (0.4–40 MPa) (Takai et al., 2008). Piezophilic growth of the strain significantly affected the stable carbon isotope fractionation of methanogenesis –$\delta^{13}C\ CH_4$) from CO_2, shifting from –34‰ to –27‰ under conventional growth conditions to < –9.4‰ at 122 °C and 40 MPa. This indicated archaeal-mediated methanogenesis in hydrothermal systems wherein CO_2 is reduced to methane (CH_4) to produce cellular energy. An extremely high abundance of molecular hydrogen (2.5 mM) in KHF fluids could serve as the primary energy source for microbial methanogenesis. Moreover, significantly low $\delta^{13}C\text{-}CH_4$ in the vent fluids (–13.8 and –18.5‰) further supported the occurrence of the process wherein biogenic methane is produced from CO_2 (Takai et al., 2004).

In the KHF, active and inactive chimney structures host habitat-specific bacterial and archaeal communities (Han et al., 2018). Culture-independent molecular studies targeting the 16S rRNA gene revealed Epsilonproteobacteria like those belonging to order Campylobacterales, Nautiliales, and Aquificae to be the most abundant bacterial operational taxonomic units (OTUs) in active chimneys (Han et al., 2018). Epsilonproteobacteria, mainly related to various genera within the Campylobacterales, have also been reported from actively venting hydrothermal chimneys from the Manus Basin back-arc spreading center (Pjevac et al., 2018). Screening of chimney-associated microbial communities has revealed functional marker genes for hydrogen oxidation (*hupSCL)*, sulfide oxidation (*sqr*), and Sox-pathway dependent sulfur oxidation (*soxB, soxAX, soxYZ*, and *soxCD*) (Pjevac et al., 2018), highlighting the importance of Epsilonproteobacteria in S cycling. Archaeal OTUs in active chimneys of KHF consisted of thermophiles showing taxonomic affinities to Archaeoglobales (utilize aromatic compounds as electron donors, and mediate Fe(III) reduction; Anderson et al., 2011; Manzella et al., 2015), Thermococcales (capable of producing Greigite, Fe_3S_4, nanocrystals on extracellular polymeric substances; Gorlas et al., 2018), Thermoprotei (use hydrogen as an energy source; Nakagawa and Takai, 2008) and Methanococcales (thermophilic H_2-consuming methanogens; Topçuoglu et al., 2016). The predominance of members of the Methanococcales in superheated hydrothermal emissions and chimney interiors, together with the other major microbial members of the Thermococcales at the KHF imply the existence of a hyperthermophilic subsurface lithoautotrophic microbial ecosystem (HyperSLiME) dominated by hyperthermophilic methanogens (Takai et al., 2004).

Chimney structures at the KHF are made up of sphalerite ((Zn,Fe)S), chalcopyrite ($CuFeS_2$), and pyrite (FeS_2) with minor barite ($BaSO_4$) and Fe oxides (Wang et al., 2012). Suzuki et al. (2004) found high cell density (10^7–10^8 cells g^{-1}) along with an abundance of magnetotactic bacteria such as *Magnetobacterium bavaricum*. They suggested that inactive chimneys provide a distinct habitat to microbes capable of thriving on reduced sulfide minerals. Characterization of bacterial communities in inactive chimney samples by Han et al. (2018) revealed that they were affiliated to *Desulfobulbus* and SAR324 (sulfate-reducing bacteria; Nakagawa et al., 2004), *Nitrosococcus* (ammonia-oxidizing bacteria; Ding et al., 2017), *Acidiferrobacter* (iron-oxidizing bacterium; Hallberg et al., 2011), Oceanospirillales (symbionts associated with hydrothermal vent gastropods, found colonizing sunken wood; Fagervold et al., 2012; Johnson et al., 2015), Alteromonadales (found on sunken wood, polycyclic aromatic hydrocarbon degraders; Fagervold et al., 2012; Sinha et al., 2019), and Thiotrichales (hydrothermal fauna symbionts; Crépeau et al., 2011). The archaeal communities from inactive chimneys mainly belonged to Woesearchaeota (formerly named DHVEG-6) and Thaumarchaeota (Han et al., 2018), which are involved in protein degradation and carbohydrate metabolism (Li et al., 2015).

Epifluorescence microscopic analysis of 4′,6-diamidino-2-phenylindole (DAPI)-stained microbial cells from ambient seawater adjacent to hydrothermal emission and in a rising plume was an order higher (10^9 cells l^{-1}) compared with normal deep seawater (Takai et al., 2004). However, flow cytometric analysis of plume samples from the KHF have revealed similar (1.77×10^7 cells L^{-1}), lower than (9.72×10^6 cells L^{-1}) or higher (2.20×10^7 cells L^{-1}) microbial abundance than at a distal reference station (0.9–1.4×10^7 cells L^{-1}) (Noguchi et al., 2015). Neutrally buoyant plumes are enriched in (trace) metals (Fe, Mn, Cu, Zn) and REEs (Haalboom et al., 2019). The fate of these substrates is influenced by microbially mediated biogeochemical reactions (Dick et al., 2009) and the binding of minerals onto organic material derived from vent biomass or *in situ* production through microbial activity (Breier et al., 2012). Microbial 16S rRNA phylotype composition showed that chemolithoautotrophs such as the SUP05 clade (*Thioglobus* sp., involved in sulfur oxidation; Marshall and Morris, 2013; Shah et al., 2019), *Methylobacter* and *Methylococcus* (methane oxidizers; Wartiainen et al., 2006; Kleiveland et al., 2012; Smith et al., 2018), and Epsilonproteobacteria thrived in KHF plumes (Noguchi et al., 2015). This finding corroborated earlier observations of Takai et al. (2004), who reported the highest proportion of Epsilonproteobacteria in KHF plume water. The KHF plume has an anomalously high H_2 concentration of up to 46.1 nmol L^{-1}. *Hydrogenimonas thermophila*, a novel thermophilic bacterium isolated from a black smoker vent orifice at the KHF, is capable of using molecular hydrogen as the sole energy source and carbon dioxide as the sole carbon source (Takai et al., 2004). Characterization of epsilonproteobacterial isolates from deep-sea hydrothermal vent systems has also revealed that they use H_2 or reduced sulfur compounds as an electron donor and O_2, nitrate, or elemental sulfur as an electron acceptor (Takai et al., 2003, 2004). Thus, an increase in SUP05 and epsilonproteobacterial phylotypes in the KHF plume is suggestive of microbially mediated H_2 consumption. The proportion of phylotypes belonging to heterotrophs such as *Alcanivorax* (mediating hydrocarbon and sulfur oxidation) were rare in hydrothermal fluid–seawater mixing zones near vents but increased in nonbuoyant plumes away from the KHF (Noguchi et al., 2015). However, the proportion of archaeal phylotypes associated with Marine Crenarchaeota Group I (MGI) were found to increase in ambient seawater adjacent to hydrothermal vents rather than in plumes (Takai et al., 2004), implying that, unlike Epsilonproteobacteria, they were not dependent on chemolithoautotrophic metabolism (Takai et al., 2003).

A considerable amount of dissolved organic compounds excreted by hydrothermal vent-associated faunal communities has been suggested to support the archaeal community. Epsilonproteobacteria have also been reported to colonize gill filaments of the hydrothermal vent gastropod *Alviniconcha* aff. *hessleri* from the KHF.

Based on compound-specific carbon isotopic analysis, inorganic carbon fixation in the epsilonproteobacterial endosymbiont was suggested to be based on the rTCA cycle (Suzuki et al., 2005). Many heterotrophic bacteria isolated from Kali chimney plumes have high multi-stressor tolerance to desiccation, peroxide exposure, UV, and gamma-ray irradiation (La Duc et al., 2007).

Longqi

The Longqi hydrothermal field (LHF) is located at 37°47′S, 49°39′E at a water depth of 2755–2785 m and is the first active vent field found on SWIR (Tao et al., 2012). The maximum temperature of hydrothermal fluids from the Longqi field is 379 °C (Table 14.1) with a pH of 3.21 (Ding et al., 2017; Ji et al., 2017; Yue et al., 2019). The field is known to be a basalt-hosted system (Tao et al., 2014). Several active vents have been located in a zone ~ 1000 m long, indicating that the area of hydrothermal activity in the Longqi field is very large (Tao et al., 2012, 2014). Hydrothermal fluids have a high concentration of chlorine when compared with ambient seawater, which is characteristic of fluid–rock interaction and phase-separation (Ji et al., 2017). High concentrations of dissolved gases and metals indicate circulation of hydrothermal fluids through a long reaction path of > 6 km involving both mafic and ultramafic lithologies (Tao et al., 2020). The hydrothermal fluids then ascend to the seafloor where they branch and expel from multiple vents (Ji et al., 2017). Endmember compositions of vents fluids from LHF arise from a single source and have shown no significant difference from those observed along the CIR (Table 14.1). This indicates that the spreading rate is not a key factor in controlling hydrothermal vent fluid chemistry (Ji et al., 2017).

Sulfide chimneys are formed as a product of high temperature (300–350 °C), hydrothermal activity, whereas Si-rich chimneys form at a fluid temperature of < 100 °C (Lei et al., 2017). The LHF is mainly constructed of chalcopyrite ($CuFeS_2$), kusachiite ($CuBi_2O_4$), pyrite (FeS_2), and manganese phosphate hydrate (Djurhuus et al., 2017). Detailed investigations have revealed that chimneys from LHF, with a fluid temperature of < 362 °C have pyrite and zinc sulfide as major components, while those with a temperature ≥ 379 °C are dominated by Bementite and Birnessite (Ding et al., 2017). In low-temperature hydrothermal chimneys on SWIR, microbial density is ~ 10^4–10^5 cells g^{-1} wet weight (Cao et al., 2014). In agreement with previous studies from hydrothermal systems elsewhere, microbial community structure analysis of chimney fragments from LHF has revealed greater bacterial diversity than that of Archaea (Ding et al., 2017) (Zhang et al., 2016). A distinct stratified pattern of microbial distribution in sulfide chimneys from SWIR has also been observed (Cao et al., 2014). *In situ* fluid temperature and gaseous components have been suggested to be the main components controlling microbial community structure (Ding et al., 2017; Lei et al., 2017). Sulfur-reducing Deltaproteobacteria dominate in the interior of the chimney (Sylvan et al., 2013), where they could be reducing sulfate to sulfide, resulting in the precipitation of metals (Cao et al., 2014). Lipid biomarkers have also supported the abundance of sulfate-reducing bacteria in sulfide chimneys (Lei et al., 2017), where they could coexist with methanogens (Sela-Adler et al., 2017) and compete for hydrogen (Hoehler et al., 1998). Epsilonproteobacteria, Gammaproteobacteria, Alphaproteobacteria, and Deltaproteobacteria and members of the phyla Bacteroidetes and Planctomycetes are the dominant bacterial lineages inhabiting the surface of sulfide chimneys (Cao et al., 2014; Ding et al., 2017). As observed in fluid/chimney samples collected from hydrothermal fields along the CIR (Kawagucci et al., 2016; Han et al., 2018) and elsewhere (Huber et al., 2010; Li et al., 2014), members within class Epsilonproteobacteria dominated the sulfur-oxidizing chemolithoautotrophic community. Sulfide-oxidizing autotrophs belonging to the genus *Sulfurovum* and the genus *Sulfurimonas* within Epsilonproteobacteria have been reported from high-temperature chimneys primarily composed of sulfide minerals (Lin et al., 2016). Sulfur-oxidizing bacteria could utilize sulfide as an energy source, leading to oxidization of sulfide to sulfate, followed by precipitation of sulfate in the outer chimney. Nitrates, metals, and hydrogen could function as electron donors or acceptors for sulfate-reducing and sulfur-oxidizing bacteria (Cao et al., 2014). Organotrophic Bacteroidetes grow as ectobionts on long, sheathed microbial filaments affiliated to the lithoautotrophic genus *Sulfurovum*. They utilize organic polymers produced by the host, thereby recycling organic matter in biofilms that grow on the surface of black smoker chimneys (Stokke et al., 2015). Members of Alphaproteobacteria, Deltaproteobacteria, and Gammaproteobacteria have also been reported to be dominant in inactive sulfide chimneys. They are thought to mediate diverse geochemical processes, including iron oxidation and nitrogen fixation ammonia oxidation, and denitrification (Li et al., 2017). Anaerobic metabolic abilities e.g., reduction of elemental sulfur to sulfide and carbohydrate fermentation are widely distributed among all significant Planctomycetes lineages, which they use for growth and survival (Elshahed et al., 2007).

Thaumarchaeota, Woesearchaeota, and Euryarchaeota were dominant archaeal lineages in LHF chimney fragments (Ding et al., 2017). Thaumarchaeota and Euryarchaeota have also been reported to colonize inactive vents (Zhang et al., 2016) and sediments (Wu et al., 2014; Wang et al., 2017) in hydrothermal fields. Thaumarchaeota, which are predominantly ammonia oxidizers (Wang et al., 2017), are abundant in Si-rich chimneys (Lei et al., 2017) and play a critical role in nitrogen cycling (Pester et al., 2011). Hyperthermophilic methanogens comprise most of the archaeal community in sulfide chimneys from the LHF (Lei et al., 2017). Euryarchaeota facilitates the anaerobic conversion of H_2, formate, acetate, methyl compounds, and simple alcohols to CH_4 and CO_2 (Nobu et al., 2016). Woesearchaeota can metabolize carbon and hydrogen under anaerobic conditions, which be might be associated with symbiotic and/or fermentation-based lifestyles (Castelle et al., 2015). Thus, the dominance of these major archaeal phyla in active chimneys is indicative of their role in biogeochemical cycling.

Hydrothermal plumes from LHF also have many bacterial and archaeal densities ranging from 10^8 to10^9 16S rRNA gene copies L^{-1}. These microbes are sourced from ambient deep seawater rather than from seafloor vent-derived niches (Dick et al., 2013; Li et al., 2016). Unlike at the CIR (Takai et al., 2004b), archaeal populations in hydrothermal plumes at the SWIR are spatially homogeneous and dominated by members of marine group I within the Crenarchaeota, which are involved in ammonia oxidation (Sintes et al., 2013). Conversely, bacterial communities in hydrothermal plumes are heterogenous in their distribution, consisting mainly of members within Alphaproteobacteria and Gammaproteobacteria (Li et al., 2016). Vent-specific genera (*Arcobacter*, *Caminibacter*, and *Sulfurimonas*) from the Epsilonproteobacteria and the SUP05 group from the Gammaproteobacteria have been reported from the LHF (Djurhuus et al., 2017). Epsilonproteobacteria are known to grow closer to the sulfide source (Patwardhan et al., 2018), but sequences from this class have not been reported from hydrothermal sediments in the vicinity of the Tiancheng vent field. Gammaproteobacteria are the most dominant microorganisms in these sediments, followed by Alphaproteobacteria and Deltaproteobacteria (Wu et al., 2014). Unlike *Epsilonproteobacteria*, metabolically versatile *Gammaproteobacteria* tend to become prevalent once the community is established (Patwardhan et al., 2018). Their abundance has been found to increase with distance from the vent area (Wang et al., 2015). Wu et al. (2014) found no overlap of bacterial OTUs (at 97% identity threshold) from hydrothermal sediments with those from previous studies on active and inactive chimney structures (Suzuki et al., 2004; Takai et al., 2004a), indicating different bacterial abundances within areas sampled in hydrothermal vent fields.

Few attempts have been made to isolate, identify and characterize bacterial strains from the SWIR. Exopolysaccharide producing novel strains such as *Alteromonas pelagimontana* sp. nov. and *Idiomarina* sp. 5.13 have been reported, and the latter strain possesses various genes for metal resistance (Sinha et al., 2017). Sequences of closely related known Mn (II)-oxidizing microorganisms (*Acinetobacter*, *Alteromonas*, *Erythrobacter*, *Halomonas*, *Marinobacter*, *Pseudoalteromonas*, *Pseudomonas*, and *Sulfilobacter*) have been retrieved in abundance from bacterial clone libraries of SWIR plume samples indicating a profusion of metal-resistant bacteria (Li et al., 2016). Gammaproteobacteria such as *Halomonas meridiana* and *Marinobacter algicola* isolated from SWIR waters can tolerate dissolved Mn concentrations up to two orders greater than in ambient seawater (Fernandes et al., 2018). They have the ability to detoxify elevated levels of Mn(II), converting it into an insoluble oxide which has similarities to the hydrothermal vein mineral Rhodochrosite. Exopolymeric material secreted by Mn(II) oxidizers acts as a nucleation site for the deposition of Mn oxide. Cell aggregates have been observed to be encrusted with microspheres (Figure 14.4). Scanning electron microscopic observations of low-temperature silica-rich deposits from the LHF have also revealed precipitation of silica spheres and Fe sulfides which is promoted and accelerated by the secretion of microbial extracellular polymer saccharide (Peng et al., 2011). A similar biomineralization style has been observed in Fe–Mn deposits from the Lau Basin (Fernandes et al., 2018). These findings revealed that bacterially mediated metal oxidation could mitigate excess levels of trace metals in hydrothermal ecosystems.

Autochthonous bacteria can contribute to a certain extent in the formation of mineral deposits along mid-oceanic ridges and have a potential for use in bioremediation and biotechnological applications (Fernandes et al., 2005, 2018). Several bacteria capable of degrading

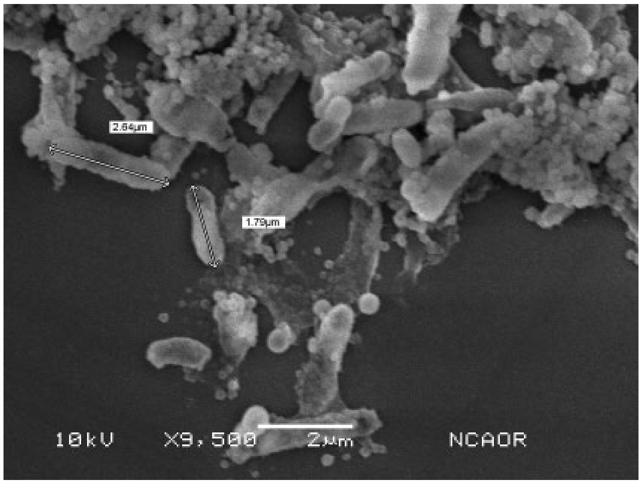

Figure 14.4 Scanning electron micrograph of Marinobacter algicola incubated in culture medium amended with 10 mmol l^{-1} Mn(II). The cells entrap Mn oxide in exopolymeric material and are encrusted with microspheres (modified after Fernandes et al., 2018) possibly formed from amorphous silica (Peng et al., 2011).

polycyclic aromatic hydrocarbons (PAH) and using them as a sole carbon source have been isolated from deep-sea waters (3946–4746 m) along the SWIR. Novel strains with PAH-degrading capabilities show close taxonomic affinities to *Alterierythrobacter*, *Citricella*, *Erythrobacter*, *Idiomarina*, *Lutibacterium*, *Maricaulis*, *Marinobacter*, *Martelella*, *Pseudidiomarina*, *Rhodobacter*, *Roseovarius*, *Salipiger*, *Sphingopyxis*, and *Stappia* spp. (Yuan et al., 2015). High-throughput DNA-based analysis of environmental samples has also shown that a considerable fraction of the microbial community along the Indian ridge system is composed of unclassified/unknown organisms (Kawagucci et al., 2016; Ding et al., 2017; Sinha et al., 2019). These findings provide an unprecedented opportunity to modify existing culturing techniques to harness pertinent microbes for bioprospecting.

The geochemical composition of hydrothermal fluids of the Dodo, Solitaire, Edmond, Kairei, and Longqi vent fields shows that basalts host all these systems. However, the Kairei fluids have high concentrations of hydrogen, and Longqi fluids have high concentrations of methane. These concentrations are quite unusual for basalt hosted system and indicates the possible fluid circulation through ultramafic rocks. Abundant populations of (hyper)thermophilic hydrogenotrophic chemolithoautotrophs are associated with Dodo, Solitaire, and Kairei fluids. In contrast, Fe/Mn-oxidizing chemolithoautotrophs belonging to *Zetaproteobacteria* or various metal-resistant genera within class Alphaproteobacteria and Gammaproteobacteria thrive on metal-rich Edmond and Longqui vent fluids. Therefore, it is evident that the fluid chemical composition and associated biology are primarily controlled by subsurface water-rock reactions. Detailed geological studies of these fields have supported the arguments. The Longqi field is located on the SWIR, whereas the other four fields, Dodo, Solitaire, Edmond, and Kairei, are located on the southern CIR. Geophysical studies have classified the SWIR as ultraslow-spreading and the southern CIR as intermediate-spreading ridges. Although the spreading rate of CIR and SWIR is different, hydrothermal systems discovered along these ridges are mostly basalt hosted. Therefore, it is perceived that the spreading rate has no role in the genesis of fluid chemical composition and associated biosphere.

14.3.2. Other Active Fields

Tiancheng

Tiancheng field is located at 63°32′E and 27°57′S; it is hosted by fractured basalts and is characterized by low-temperature (up to 13.2 °C) diffuse flow. Recent studies on trace metal in Tiancheng hydrothermal plumes (both buoyant and non-buoyant) show that the majority (75–100%) of the dissolved manganese is present in the soluble phase (< 1 kDa). Whereas more than 66% of dissolved Fe was removed in the buoyant stage of the plume, and 54–95% of the Fe is present as the colloidal phase in the buoyant plume (Fang and Wang, 2021). There is a widespread occurrence of hydrothermal fauna such as mussels, gastropods, crabs, shrimps, barnacles, and anemones on the seafloor (Chen et al., 2018). A new population of the scaly-foot snail *C. squamiferum* has been reported from the vent field. It has reddish-brown coloration from zinc sulfide deposits on the surface of its sclerites, unlike those at the Kairei field, which have black scales infused with iron sulfide nanoparticles. Scales lacking iron but still enriched in sulfur may be adapted to remove sulfur metabolites from their bodies (Sun et al., 2020).

Pelagia

Pelagia field is located at 26°S and 71°E of the SEIR (Han et al., 2018). The high-temperature fluids (332–256 °C) are highly enriched in dissolved Fe, Si, K, Li, Mn, and Zn, and apparently not affected by supercritical phase separation in the subsurface (Noowong et al., 2021). Chimneys are predominantly covered by swarms of hydrothermal vent endemic shrimps (*R. kairei*) and hydrothermal fluids have been observed to emanate from open fissures on the seafloor. Diffuse hydrothermal fluid and plume water samples in the Pelagia area harbor up to 107 microbial cells L^{-1} (Han et al., 2018). Active chimneys in the vent field appear to host habitat-specific microbial communities with low or no resemblance to known species. The bacterial community in the Pelagia active chimneys has been found to be dominated by OTUs classified as Epsilonproteobacteria, particularly the orders Nautiliales and Aquificae. These microbes can reduce sulfur to sulfide, thereby contributing to the formation of metal sulfides (Han et al., 2018). Dense colonies of endemic vent species such as mussels and other benthic communities have also been observed near the outlet of fissures.

Wocan

The Wocan Hydrothermal Field (WHF) was discovered in 2013 and has two hydrothermal sites (Wocan-1 and Wocan-2) on the axial volcanic ridge located at 6°22′N, 60°31′E on the slow-spreading CR (Wang et al., 2017). Iron- and copper-rich sulfides (Wang et al., 2017) along with the Fe–Si–Mn-oxyhydroxides (Popoola et al., 2019a) and metalliferous sediments (Popoola et al., 2019b) have been recovered from this field. The recovered hydrothermal precipitates can be classified into (i) Cu-rich chimneys, (ii) Cu-rich massive sulfides, (iii) Fe-rich massive sulfides, and (iv) silicified massive sulfides. Based on mineralogy and geochemistry of sulfide deposits, Wang et al. (2017) have inferred that Wocan-1 has undergone a cycle of heating with Cu-rich chimney growth and subsequent cooling, followed by late seafloor weathering, while Wocan-2 has undergone intermediate- to high-temperature mineralization followed by intense silicification of sulfides.

Onnuri

The active Onnuri vent field (OVF) was discovered at 11°24.9′S, 66°25.4′E at a water depth of 1990–2170 m. Disseminated sulfide assemblages with barite, altered rocks, Fe oxide crust, and vent organisms (hairy snails, mussels, barnacles, shrimps, and crabs) have been reported to be widely distributed around the field. Isolation of *Thermococcus indicus* sp. nov., a Fe(III)-reducing hyperthermophilic archaeon has suggested the presence and abundant occurrence of a thermophilic iron-reducing microbial population in the Onnuri vent field (Lim et al., 2020). Thin greenish layers of Cu-bearing secondary minerals were observed in breccia-type sulfides, which imply that: (i) the hydrothermal system might be affected by high-temperature fluids at least beneath the site, although plume data indicate low-temperature, diffuse venting is dominant; or (ii) high-temperature venting was present in the past, but the site is now waning (Kim et al., 2020).

Old City

The Old City hydrothermal field (OCHF; 27° 50.1′S; 64°35.1′E) along the SWIR (Sauter et al. 2013; Lecoeuvre et al., 2018) is a serpentinite-hosted hydrothermal site located ~3100 m below sea level. It is characterized by extremely slow and diffuse hydrothermal fluid flow. Carbonate–brucite chimneys at the OCHF are similar to those observed at the Lost City hydrothermal field (LCHF) along the mid-Atlantic ridge (Lecoeuvre et al., 2021). Metagenomic analysis of five chimney samples from OCHF has revealed significant taxonomic and metabolic heterogeneities among microbial populations (Lecoeuvre et al., 2021). Although formate- and CO-metabolizing microorganisms and sulfur-metabolizing bacteria are widespread, variable geochemical conditions with mixed but variable influences of reducing hydrothermal fluids has resulted in strong differences in microbial populations between chimneys. Nevertheless, similarities in bacterial and archaeal lineages were reported between the OCHF and LCHF chimney samples. The exteriors of less active or inactive chimneys at these hydrothermal fields are dominated by Proteobacteria that show metabolic capabilities for aerobic respiration, CO_2 fixation through the Calvin–Benson–Bassham cycle, and sulfur and nitrogen metabolism (Lecoeuvre et al., 2021).

Different sets of scientific information are available from different vent fields, and more detailed studies (chemical and biological properties of hydrothermal fluid along with geological background and vent organisms) are required to understand these systems.

14.3.3. Inactive Vent Fields

Sonne

The first hydrothermal field in the entire Indian Ocean was the SONNE field (Pluger, 1990), and the “MESO zone” at 23°21′S, 69°15′E is the area where massive sulfides were recovered in the MESO zone (Halbach et al., 1995). The MESO zone, which covers an area of about 0.6 km^2, is located at a water depth of 2850 m, and has sulfides that have formed over a period of at least 30,000 years. These sulfides are composed mainly of pyrite, marcasite, and chalcopyrite with traces of sphalerite, but they also contain minor amounts of amorphous silica (**Münch** et al., 1999). Chimneys show high concentrations of Cu and Fe _(>40 wt.%) followed by Zn (1 wt.%) and trace element contents such as Co up to 0.24 wt%. However, hydrothermal activity at the MESO zone ceased about 10 000 years ago (Lalou et al., 1998).

Yokoniwa

Yokoniwa hydrothermal field (YHF), which was identified in 2009, is an ultramafic-hosted system located on top of the Yokoniwa Rise (YR) and is very close to the Kairei field (Okino et al., 2015, Fujii et al., 2016). Hydrothermal sulfides and small dead chimneys were observed. The hydrothermal activity of the YHF was almost ended as indicated by weak venting of low-temperature fluids (<5°C) during submersible surveys. Serpentinized peridotite is extensively exposed along with small quantities of gabbro, dolerite, and basalt (Okino et al., 2015; Sato et al., 2015).

Mount Jourdanne

In 1998, the Mt. Jourdanne hydrothermal field was discovered at 27°51′S, 63°56′E and massive sulfide and chimney samples were collected (Münch et al., 2001). The sulfide samples recovered from Mount Jourdanne are classified as chimneys, mounds, and hydrothermal breccias (Nayak et al., 2014). The chimneys consist mainly of sphalerite and less chalcopyrite, set in matrix of late amorphous silica. In contrast, the mounds are dominated either by Fe sulfides (pyrite) or by a mixture of pyrite and chalcopyrite with less sphalerite, pyrrhotite, amorphous silica, and barite. The breccias consist of silicified basaltic material that is impregnated with sulfides and contain small chimney fragments within a matrix of low-temperature minerals such as sphalerite and pyrite. In addition, breccias also contain late-stage realgar, boulangerite, galena, Pb–As sulfosalts, and barite. Based on the different mineralogical associations, Nayak et al. (2014) have observed different thermal episodes ranging from black smoker mineralization conditions to cessation of the hydrothermal activity at Mt. Jourdanne.

Tianzuo

The Tianzuo hydrothermal field is an inactive sulfide field at 27°57′S, 63°32′E, which is hosted by ultramafic rocks and controlled by detachment fault (Tao et al., 2014, Chen et al., 2018). Polymetallic sulfide, reddish-brown iron hydroxide, polymetallic mud, and peridotite samples have been recovered from this field (Cao et al., 2021). No apparent mineralogical zonation was observed in the sulfides, which are dominated by marcasite and a small amount of pyrite (Py), opal, and covellite. Severe sulfide weathering alteration was found, and Fe oxyhydroxides were observed along the fissures. Cao et al. (2021) demonstrated that the composition of sulfides is controlled by multistage hydrothermal activity and the pervasive transform faults apart from the basement rock composition.

Yuhuang-1

Hydrothermal sulfides at Yuhuang-1 are the shallowest deposits (1400 m) on the SWIR at 49.26°E and 37.94°S (Han et al., 2010, Tao et al., 2014, Yu et al., 2021). The sulfide samples mainly consist of sphalerite, wurtzite, pyrite, marcasite, chalcopyrite, and secondary copper minerals and are classified as (i) Fe-rich sulfides, (ii) Zn-rich sulfides, and (iii) Cu-rich sulfides (Yu et al., 2021). The total volume of sulfide-rich mounds is calculated to be approximately 10.6×10^6 t. This includes at least ~7.5×10^5 tons of copper and zinc and ~18 tons of gold. The distribution and content of sulfide-rich deposits in the Yuhuang-1 hydrothermal field are composed of two areas ~ 500 m apart: the southwest sulfide area (SWS) and the northeast sulfide area (NES).

Duanqiao-1

Sulfides recovered from Duanqiao-1 hydrothermal field at 50°24′E and 37°39′S are mainly dominated by pyrite and sphalerite with a small amount of chalcopyrite and trace amounts of galena (Tao et al., 2012). Based on the detailed mineralogical studies of the sulfides, mineralization processes were divided into two main stages: (i) the medium–high-temperature stage and (ii) the medium–low-temperature stage (Zhang et al., 2018). Dating of the relict chimney and massive sulfides reveal four main episodes: (i) 68.9–84.3 thousand years, (ii) 43.9–48.4 thousand years, (iii) 25.3–34.8 thousand years and (iv) 0.7–17.3 thousand years, and about 84.3 (±0.5) thousand years ago; hydrothermal activity might have started and ceased about 0.737 (±0.023) thousand years ago (Yang et al., 2017). Sediments recovered from this field show mainly pelagic fractions (carbonate ooze) with minor clay contents, basaltic debris, Fe–Mn oxyhydroxides, and hydrothermal components (Liao et al., 2019). High concentrations of Cu, Pb, Zn, and Co and higher Cu/Fe and Zn/Fe ratios promote the precipitation of Cu sulfides first in the close proximity of the discharge area and followed by Cu, Zn, and Fe sulfides, and Fe-Mn oxyhydroxides with increasing distance from the source (Liao et al., 2019).

A total of 22 hydrothermal fields have been discovered so far along the Indian mid-oceanic ridge system. The majority of these fields are located along the SWIR and CIR. Among them, 10 fields are located along the SWIR and named Yuhuang-1 (49°16′ E/37°56′S), Longqi (49°39′E/37°47′S), Duanqiao-1 (50°24′E/37°39′S), 50°56′E carbonate field (50°56′E/37°37′S), 51°19′E field (51°19′E/37°27′S), 53°15′S field (53°15′E/36°60′S), Tiancheng (63°32′E/27°57′S), Tianzuo (63°31.8′E/27°57′S), Mount Jourdanne (63°56′E/27°51′S) and Old City (64°35.1É/27°50.1′S). Another 10 fields have been discovered along the CIR and named as Kairei (25°19.23′S/70°02.42′E), Yokoniwa (25°16′S/70°04′E), Edmond (23°52.68′S/69°35.80′E), Sonne (23°21′S/69°15′E), Solitaire (19°33.413′S/65°50.888′E), Dodo (18°20.1′S/65°17.9′E), Onnuri (11°24.9′S/66°25.4′E), 9°48.9′S field (9°48.9′S/66°40.6′E), 9°47.5′S field (9°47.5′S/66°41.9′E) and 8°10.1′S field (8°10.1′S/68°08.2′E). Only two fields have been discovered along the CR and SEIR and these have been named Wocan (6°22′N/60°31′E) and Pelagia (26°S/71°E).

14.3.4. Hydrothermal Plume Signatures in Water Column/Sediments/Ferromanganese Crusts

Several studies on water column tracers (both physical and chemical) in the CIR provide indirect evidence of hydrothermal activity in the region (Jean-Baptiste et al., 1992; Gamo et al., 1996, 2001; Kawagucci et al., 2008; Kumagai et al., 2008; Nakamura et al., 2009, 2012; Son et al., 2014; Ray et al., 2020). While some studies have focused on already discovered vent fields such as Dodo, Solitaire, Edmond, and Kairei, the others infer the existence of plume signatures in other unexplored areas. Very few reports are available on water column anomalies (German et al., 1998; Bach et al., 2002; Boulart et al., 2017) for active venting along with an inactive hydrothermal field (Tao et al., 2014; Han et al., 2018) in the SWIR and SEIR. To date, only one mega-event plume (CR2003; Murton et al., 2006) has been reported from the Carlsberg Ridge. This plume spread about 70 km (between 61°30E, 5°41′N and 60°33′E, 6°20′N) and additional small-scale events have been observed by Ray et al., (2008). In addition to this event plume, the first chronic plumes from two different locations have been reported at 3°42′N and 3°41.5′N (Ray et al., 2012, 2017). In subsequent years, a Chinese research team has recovered hydrothermal sulfides from this region (Tao et al., 2013).

Signatures of hydrothermal activity in ferromanganese crusts and sediments along the Indian ridge system and from other parts such as the back-arc basin (Andaman) and the abyssal basin (Central Indian Ocean Basin) have been reported by Nath et al., 1992, 1997; Rao et al., 1996; Kuhn et al., 1998, 2000; Kurian et al., 2008; Mascarenhas-Pereira and Nath, 2010; Kamesh Raju et al., 2012a; Surya Prakash et al., 2012; 2020; Kalangutkar et al., 2015; Li et al., 2016, 2017; Liao et al., 2018; Yu et al., 2018; Sinha et al., 2019; Agarwal et al., 2020.

14.3.5. Vent Fauna Associated with Hydrothermal Vents in the Indian Ocean

Studies on the biodiversity and biogeography of Indian Ocean vent fauna were initiated only after discovering the Kairei vent field (Van Dover et al., 2001). Even though hydrothermal vents along the CIR and SWIR are located within a limited area, they are considered to be reasonably diverse in terms of biological communities associated with them (Nakamura and Takai, 2015b). The diversity of vent-specific communities has been described by many researchers (Haymon et al., 1993; Hashimoto et al., 2001; Van Dover et al., 2001; Nakamura et al., 2012; Beedessee et al., 2013; Chen et al., 2015; Copley et al., 2016; Watanabe et al., 2018; Zhou et al., 2018; Jang et al., 2020; Sun et al., 2020). Based on published reports ~100 macrobenthic and megabenthic species/genera occur at the eight known active hydrothermal vent sites in the Indian Ocean (Table 14.2). The benthic fauna comprises 38 families belonging to eight phyla. The most dominant phylum in terms of the number of species/genera is Annelida, with 28 (29.2%) taxa belonging to eight families. Arthropoda is the second dominant phylum in order of faunal abundance, with 26 (27.1%) described/identified taxa belonging to nine families. Mollusca is the third most dominant phylum of vent fauna in the Indian Ocean (Table 14.3) and is represented by 25 (26.0%) species. Echinodermata is represented by three families (Chiridotidae, Prerasteridae, and Synaptidae). Cnidaria is represented by two families, whereas Nemertea and Platyhelminthes are represented with one family each. Chordata is represented by five families of ichthyofauna (fish). Of these, three families (Synaphobranchidae, Zoarcidae, and Macroudidae) were reported previously from the KHF (Hashimoto et al., 2001; Watanabe and Beedessee, 2015), and the families Ophidiidae and Notocanthidae were recently reported from the newly discovered Tiancheng hydrothermal vent field along the SWIR (Zhou et al., 2018; Sun et al., 2020). As shown in Table 14.3, most of the vent-dominant molluscs, crustacean, and annelid taxa are recorded from both CIR and SWIR vent fields. However, slightly higher benthic diversity (52%) has been reported from the four vent fields of the CIR systems (Figure 14.5). At the same time, with >35 confirmed benthic faunal taxa (genera/species), the KHF remains the most diverse among all the known active vent fields in the Indian Ocean. However, >30 vent specific benthic taxa have been reported from the Longqi vent field, making Longqi the most diverse and scientifically exciting vent field on the SWIR. Interestingly, most of the faunal taxon occurs concomitantly, suggesting a possible biogeographic and potential genetic connectivity between hydrothermal vent faunal communities along the CIR and SWIR (Sun et al., 2020). Although hydrothermal vent fauna of the Indian Ocean represents some of very unusual endemic species such as the Scaly-foot gastropod *C. squamiferum*, the biodiversity of this region is poorly understood compared with the well-studied Pacific and Atlantic vent systems (Sun et al., 2020). Nevertheless, analogous to the fauna of the other vents, a number of the species are believed to be endemic and are known to occur within the area of individual vents (Chen et al., 2015). In contrast, the vent crab *A. rodriguezensis*, vent shrimps *Rimicaris kairei*, and *M. indica*, the deep-sea mussel *B. marisindicus* and the Scaly-foot gastropods (*C. squamiferum* and *Alviniconcha* sp.) and barnacle (*Neolepas* sp.) are found at both the CIR and SWIR vent fields (Figure 14.6): they are among the most widely distributed vent species in the Indian Ocean (Nakamura et al., 2012; Copley et al., 2016; Zhou et al., 2018; Ryu et al., 2019; Jang et al. 2020; Kim et al., 2020; Sun et al., 2020). According to recent studies, the larvae of vent crab *A. rodriguezensis* can disperse among hydrothermal vent fields using surface currents (Beedessee et al., 2013). Moreover, phylogenetic and fossil analysis of hydrothermal vent stalked barnacles belonging to genus *Neolepas* is capable of long-distance migration (Watanabe et al., 2018). As these vent barnacles are widely distributed among different oceanic provinces and are the most conspicuous organisms in deep-sea hydrothermal vents (Herrera et al., 2015), they are considered excellent model organisms for studying the connectivity and biogeographic patterns in deep-sea chemosynthetic fauna.

Similarly, phylogenetic analysis of the vent shrimp *R. kairei* showed close lineages to the *Rimicaris exoculata* of the MOR vent field (Beedessee et al., 2013). Larvae of some vent species are known to survive away from the vent field for long periods (Herring and Dixon, 1998). Some shrimp larvae from Alvinocarididae family presumably feed on photosynthetic-based food, especially during their long dispersal periods (Beedessee et al., 2013). It is quite likely that some of the shrimp's species belonging to the family Alvinocarididae generally inhabit deep-sea hydrothermal vent areas, plausibly connected with cold-seep species present at the nearby cold-seep environments.

Table 14.2 Updated list of benthic fauna associated with Indian Ocean vent fields.

			Central Indian Ridge					Southwest Indian Ridge		
Phylum	Family	Species	Onnuri	Dodo	Solitaire	Emmond	Kairei	Tiancheng	Duanqiao	Longqi
Cnidaria	Actinostolidae	*Marianactis* sp.	+	+	+	+	+	+		
		Actinostolid sp. tiancheng						+		
		Actinostolid sp. sp. SWIR								+
	Cerianthidae	Cerianthidae sp.					+			
Arthropoda	Bythograeidae	*Austinograea rodriguezensis*	+	+	+	+	+	+		
	Kiwaidae	*Kiwa* sp. SWIR							+	+
	Alvinocarididae	*Rimicaris kairei*	+	+	+	+	+			+
		Chorocaris sp			+					+
		Mirocaris indica			+	+	+	+		+
		Alvinocaris solitaire			+					
	Galatheidae	*Munidopsis* sp.			+		+			
		Munidopsis sp. SWIR								+
		Galathidae indet						+		
	Ammotheidae	*Sericosura heteroscela*							+	+
		Sericosura bamberi							+	
		Sericosura n.sp SWIR							+	
	Dirivultidae	Dirivultidae indet						+		
		Aphotopointius limatulus	+							
		Aphotopointius Kiost	+							
		Aphotopointius muricatus	+							
		Benthoxynus constrictus	+							
		Stygiopontius spinifer	+							
		Stygiopontius horridus	+							
		Stygiopontius geminus	+							
		Stygiopontius quadripaxillifer	+							
	Schminkepinellidae	*Barathricola thermophilus*	+							
	Eolepadidae	*Neolepas marisindica*			+		+	+		
		Neolepas sp.						+	+	+
	Chionelasmatidae	*Eochionelasmus coreana*			+					
		Eochionelasmus sp.			+		+			

Mollusca	Mitilidae	*Bathymodiolus marisindicus*	+	+		+	+	+	+
		Gigantidas verijenhoeki	+						
	Lepetodrilidae	*Lepetodrilus* sp.		+		+			
		Lepetodrilus n. sp SWIR						+	+
		Pseudorimula sp. SWIR					+		+
		Pseudorimula sp.				+			
	Neolepetopsidae	*Eulepetopsis* sp.		+		+	+		
		Pseudorimula sp.					+		
	Peltospiridae (Scaly foot)	*Chrysomallon squamiferum*		+		+	+	+	+
		Gigantopelta aegis						+	+
		Dracogyra subfuscus							+
		Lirapex politus							+
	Phenacolepadidae	*Shinkailepas* sp.		+		+			
	Provannidae	*Alviniconcha* aff. *hessleri*		+	+	+			
		Alviniconcha cf. *marisindica*					+		
		Desbruyeresia cf. *marisindica*					+		
		Desbruyeresia sp.		+		+		+	
	Skeneidae	*Bruceiella* sp.				+			
	Raphitomidae	*Phymorhynchus* sp.		+	+	+			
		Phymorhynchus sp. *Tiancheng*					+		
		Phymorhynchus n. sp. SWIR							+
	Simrothiellidae	*Helicoradomenia*? sp.				+			
	Sutulizonidae	*Sutulizona* sp.				+			
		Slit limpet sp. 1				+			
		Slit limpet sp. 2				+			
Annelida	Alvinellidae	Alvinellid gen. et sp.		+					
	Ampharetidae	*Amphisamytha* sp.				+			
		Amphisamytha n. sp. 1							+
		Amphisamytha n. sp. 2							+
	Amphinomidae	*Archinome* cf. *jasoni*		+		+			+
	Capitellidae	Capitellid sp. 1				+			
	Dorvilleidae	*Ophryotrocha* sp.				+			
		Cf. *Ophryotrocha* sp.					+		
		Ophryotrocha jiaolongi							+
	Hesionidae	Hesionid sp. 1				+			
		Hesionid sp. 2				+			
		Hesiolyra cf. *bergi*						+	+
		Hesionidae sp. Indet							+

(*Continued*)

Table 14.2 (Continued)

Phylum	Family	Species	Central Indian Ridge					Southwest Indian Ridge		
			Onnuri	Dodo	Solitaire	Emmond	Kairei	Tiancheng	Duanqiao	Longqi
	Polynoidae	*Branchinotogluma* sp.					+			
		Branchinotogluma bipapillata						+	+	+
		Branchipolynoe longqiensis								+
		Branchipolynoe sp.1			+	+	+			
		Branchipolynoe Sp. 2						+	+	+
		Harmothoe? sp.					+			
		Levensteiniella? sp					+			
		Polynoidae sp3 sensu						+		
		Peinaleopolynoe n. sp. Dragon							+	+
		Polynoidae n. gen.							+	
		Polynoidae sp. 1							+	+
		Polynoidae sp. 2								+
		Polynoidae sp. 3						+		
	Spionidae	*Prionospio* sp.					+			
		Laonice sp SWIR								+
		Prionospio cf. *unilamellata*								+
Echinodermada	Chiridotidae	*Apodacean* gen. et sp.			+					
		Chiridota sp.						+		
		Chiridota heheva								+
	Prerasteridae	Prerasteridae indet								
	Synaptidae	Gen. sp					+			
Nemertea		Unidentified			+		+			
Platyhelminthes		Unidentified			+		+			
Chordata	Synaphobranchidae						+			
	Zoarcidae						+			
	Ophidiidae	Ophidiidae indet						+		
		Ophidiidae sp						+		+
	Notacanthidae	cf. *Polyacanthonotus* sp.						+		
	Macroudidae	Macrouridae gen. et sp.			+			+		

Central Indian Ridge data from: Van Dover et al. (2001), Nakamura et al. (2012), Beedessee et al. (2013), Ryu et al. (2019), Jang et al. (2020), Kim et al., (2020), and other relevant reports. Southwest Indian Ridge (SWIR) data from: Copley et al., (2016), Zhou et al. (2018); Sun et al. (2020), and other relevant reports.

Table 14.3 Details of the hydrothermal vent fauna in the Indian Ocean based on described taxa.

Phyllum	No. of families	Percentage based on total known families	No. of taxa (species/ genera)	Percentage based on total known taxa
Cnidaria	2	5.1	4	4.1
Arthopoda	9	23.1	27	27.6
Mollusca	10	25.6	25	25.5
Annelida	8	20.5	29	29.6
Echinodermata	3	7.7	5	5.1
Nemertea	1	2.6	1	1.0
Platyhelminthes	1	2.6	1	1.0
Chordata	5	12.8	6	6.3
	39	100	98	100

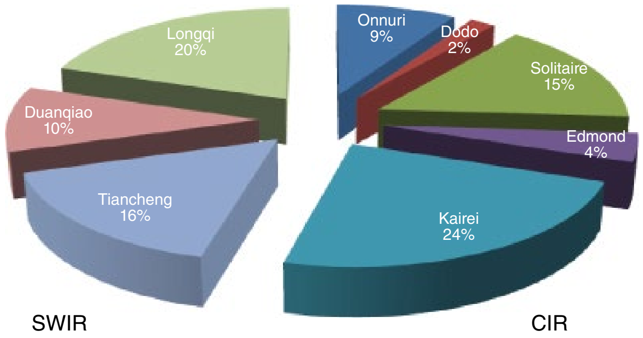

Figure 14.5 Benthic faunal richness (%) at each known vent field and comparison between CIR and SWIR vents fields. Values are based on described benthic species associated with hydrothermal vents in the Indian Ocean. Data source as shown in Table 14.2.

14.4. NATURE OF VENT-ASSOCIATED CHEMOAUTOTROPHS: ARE THEY LINKED WITH COLD-SEEP ECOSYSTEMS IN THE INDIAN OCEAN?

Mid-oceanic ridges are known to be the major source and extensive spread of hydrothermal helium, iron, and manganese in the Indian Ocean (Srinivasan et al., 2004; Nishioka et al., 2013; Vu and Sohrin, 2013; Takahata et al., 2018; Chinni et al., 2019). Recent studies on the biodiversity of the Indian Ocean hydrothermal vents from the Tiancheng field at SWIR show similarities with the Kairei and Edmond vent fields at CIR (Sun et al., 2020). Further, geochemical studies on ferromanganese crusts (Surya Prakash et al., 2020) along the Indian mid-oceanic ridges show along-ridge similarities and possible extension of deep water connectivity from south to north and follow the general bottom water flow (Antarctica Bottom Water and North Atlantic Deep Water; Kumar and Li, 1996; Wilson et al., 2012). Helium isotope studies in the Indian Ocean have identified four primary sources: (i) the mid-oceanic ridge, (ii) the Gulf of Aden, (iii) the convergent margin in the eastern Indian Ocean, and (iv) Indonesia through flow (Srinivasan et al., 2004). In addition, clockwise seawater circulation in the Northwestern Indian Ocean is responsible for the enrichment of hydrothermal helium (from the Gulf of Aden) in the Arabian Sea (Takahata et al., 2018). Similarly, we anticipate that anticlockwise seawater circulation in the eastern Indian Ocean may bring the volcanic inputs from the Indonesian Archipelago reported in the water column (Alibo and Nozaki, 2004). Therefore, in the eastern continental margin of India, the hydrothermal components (chemical and microbiological) can be expected from mid-oceanic ridges, the Andaman Sea, or Indonesia through flow.

Recent phylogeny, molecular, and fossil studies of newly described vent barnacle *Neolepas marisindica*, which is widely distributed in the Indian Ocean ridges, indicates that the genus *Neolepas* could have migrated to the Indian Ocean from the southern Pacific Ocean (Watanabe et al. 2018). Moreover, shrimp larvae from the Alvinocarididae family could presumably be feeding on photosynthesis-based food, especially during their long dispersal periods (Beedessee et al., 2013). Thus, it is quite likely that some of the species belonging to the family Galatheidae (crabs), Eolepadidae (barnacles), and Mitilidae (mussels) that generally inhabit deep-sea hydrothermal vent areas plausibly occur concurrently at nearby cold seep environments (Table 14.4) and hence are genetically interconnected. Detailed genomic studies of cold-seep communities along with detailed water column hydrothermal tracer-based (both chemical and microbiological) investigations are required to establish ecosystem connectivity between hydrothermal vents and cold-seep in the Indian Ocean.

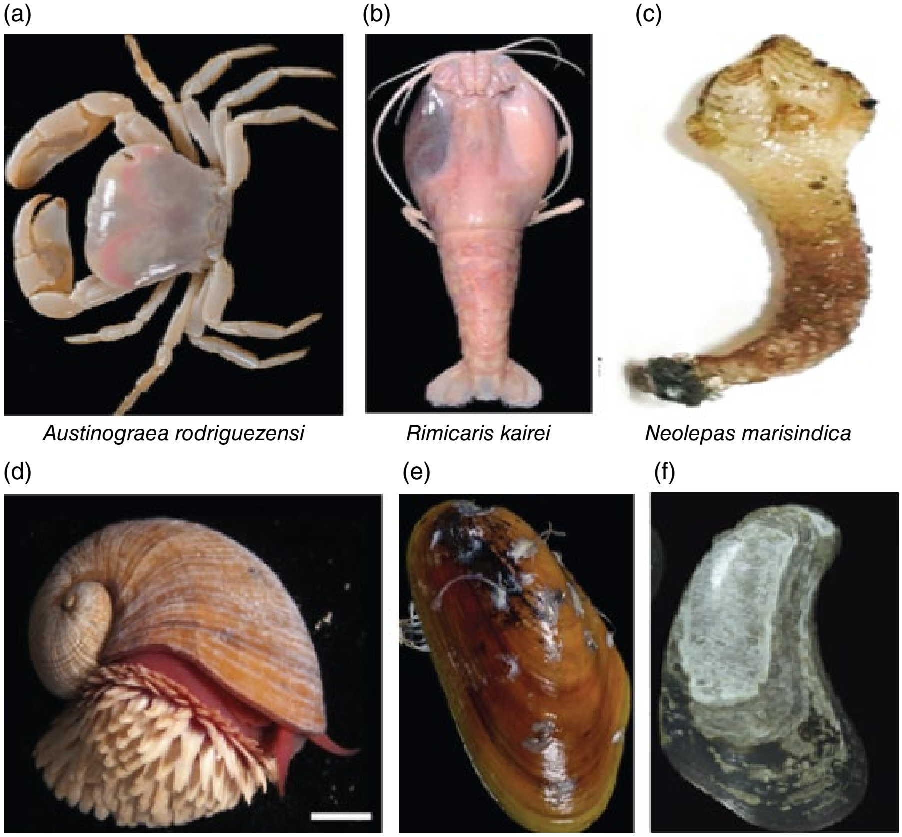

Austinograea rodriguezensi *Rimicaris kairei* *Neolepas marisindica*

Chrysomallon squamiferum *Bathymodiolus marisindicus* *Gigantidas vrijenhoeki*

Figure 14.6 Vent fauna reported from the Central Indian Ridges (CIR) and Southwest Indian ridges (SWIR) vent fields. From: Sun et al. (2020) (a,e); Nakamura et al. (2012), (b,d); Ryu et al (2019), (c); Jang et al. (2020), (f).

Table 14.4 List of the closely matching hydrothermal vent and cold-seep fauna from the Indian Ocean[a].

		Seep fauna (KG Basin, Bay of Bengal)[a]	Vent fauna (Indian Ocean)
Phylum	Family	Species/genus	Species/genus
Arthropoda	Galatheidae	Galatheidae sp	
	Munidopsidae	Munidopsidae sp.	*Munidopsis* sp.
	Eolepadidae	*Neolepas* sp.	*Neolepas marisindica*
Mollusca	Bivalvia–Vesicomyidae	*Calyptogena magnifera*	
	Thuasiridae	*Conchocele* sp.	
	Solemyida	*Acharax* sp.	
	Pectinidae	*Pectin* sp.	
	Mitilidae	*Bathymodiolus* sp.	*Bathymodiolus marisindicus*
	Gastopoda–Provannidae	Provannidae	*Alviniconcha marisindica* *Desbruyeresia marisindica*
	Phenacolepadidae, Neritoidae	*Neritid* sp.	*Shinkailepas* sp.
	Lepetodrilidae		*Lepetodrilus*
Annelida	Polychaeta–Siboglinidae	*Sclerolinum* sp.	
	Glyceridae	*Glycera* sp.	
	Serpulidae	*Serpulidae* sp.	
	Polynoidae	Branchipolynoe seepensis	Branchipolynoe loggiensis
Echinodermada	Ophiuroidea	*Amphiodia* sp	

[a] Mazumdar et al. (2019). Central Indian Ridge data from: Van Dover et al. (2001), Nakamura et al. (2012), Beedessee et al. (2013), Ryu et al. (2019), Jang et al. (2020), and Kim et al. (2020, and other relevant reports. Southwest Indian Ridge data from Copley et al. (2016); Zhou et al. (2018), Sun et al. (2020) and other relevant reports.

14.5. CONCLUSION

The Indian mid-oceanic ridge system has varying spreading rates with ultraslow (Southwest), slow (Carlsberg), and intermediate (Southeast and Central Indian Ridges). This MOR hosts hydrothermal vents with diverse geochemical compositions, microbial biodiversity, and fauna. The CIR is relatively well explored compared with other ridges with nine hydrothermal fields discovered so far. The geochemical composition of fluids from Dodo, Solitaire, Edmond, Kairei, and Longqi vent fields indicates that they are basalt-hosted systems. However, only Kairei and Longqi fluids are enriched in hydrogen and methane because of mafic–ultramafic lithological influence. A high abundance of (hyper)thermophilic hydrogenotrophic chemolithoautotrophs has been observed to be associated with the Kairei fluids, which are enriched in hydrogen concentrations. In contrast, fluids from Edmond and Longqi are enriched in metal content. Extensive microbial mats mainly consisting of metal oxidizing chemolithoautotrophs showing taxonomic similarities to Zetaproteobacteria (as observed at Loihi seamount) have been recorded at the Edmond field. The geochemical composition of vent fluids and associated microbes inhabiting these extreme environments seems to be controlled mainly by subsurface water–rock interactions, and the spreading rate of the ridge has no significant role to play. Both the CIR and SWIR vent fields have similar vent fauna, for example, the crab *A. rodriguezensis*, vent shrimp *R. kairei*, and *M. indica*, the deep-sea mussel *B. marisindicus*, the scaly-foot gastropods (*C. squamiferum, Alviniconcha* sp.), and the barnacle (*Neolepas* sp.). Significant inter-ridge connectivity can thus be inferred. Further, chemosymbiont bearing bivalves, polychaetes, and gastropods have also been discovered in cold-seep methane hydrates in the eastern Indian continental shelf. The similarity in the fauna of hydrothermal vents and cold-seep in the Indian Ocean raises the question of whether the two ecosystems are interconnected. Genomic studies of cold-seep fauna along with the water column hydrothermal tracer studies (both chemical and microbial) may provide the link between these two geographically distant systems.

ACKNOWLEDGMENTS

The authors thank the Director, ESSO-National Centre for Polar and Ocean Research, Ministry of Earth Sciences, Goa, for his encouragement. The authors are also grateful to the Editors of *Systems Biogeochemistry of Major Marine Biomes* for their invitation to contribute this chapter and to two anonymous reviewers for a thorough review. This is NCPOR contribution number B-2/2021-22.

REFERENCES

Agarwal, D.K., Roy, P., Prakash, L.S. et al. (2020). Hydrothermal signatures in sediments from eastern Southwest Indian Ridge 63°E to 68°E. *Marine Chemistry 218*: 103732. https://doi.org/10.1016/j.marchem.2019.103732

Akerman, N.H., Butterfield, D.A. and Huber, J.A. (2013). Phylogenetic diversity and functional gene patterns of sulfur-oxidizing subseafloor *Epsilonproteobacteria* in diffuse hydrothermal vent fluids. *Frontiers in Microbiology 4*. https://doi.org/10.3389/fmicb.2013.00185

Alibo, D.S. and Nozaki, Y. (2004). Dissolved rare earth elements in the eastern Indian Ocean: chemical tracers of the water masses. *Deep Sea Research Part I: Oceanographic Research Papers 51* (4): 559–576.

Anderson, I., Risso, C., Holmes, D. et al. (2011). Complete genome sequence of *Ferroglobus placidus* AEDII12DO. *Standards in Genomic Sciences 5* (1): 50–60. https://doi.org/10.4056/sigs.2225018

Bach, W., Banerjee, N.R., Dick, H.J. et al. (2002). Discovery of ancient and active hydrothermal systems along the ultra-slow spreading Southwest Indian Ridge 10°–16°E. *Geochemistry, Geophysics, Geosystems 3* (7): 1–14.

Beedessee, G., Watanabe, H., Ogura, T. et al. (2013). High connectivity of animal populations in deep-sea hydrothermal vent fields in the central Indian ridge relevant to its geological setting. *PLoS ONE 8* (12): https://doi.org/10.1371/journal.pone.0081570

Bernardino, A.F., Levin, L.A., Thurber, A.R. et al. (2012). Comparative composition, diversity and trophic ecology of sediment macrofauna at vents, seeps and organic falls. *PLoS ONE 7* (4): e33515https://doi.org/10.1371/journal.pone.0033515

Boulart, C., Briais, A., Chavagnac, V. et al. (2017). Contrasted hydrothermal activity along the South-East Indian Ridge (130°E–140°E): From crustal to ultramafic circulation. *Geochemistry, Geophysics, Geosystems 18* (7): 2446–2458. https://doi.org/10.1002/2016GC006683

Breier, J.A., Toner, B.M., Fakra, S.C. et al. (2012). Sulfur, sulfides, oxides and organic matter aggregated in submarine hydrothermal plumes at 9°50′N East Pacific Rise. *Geochimica et Cosmochimica Acta 88*: 216–236. https://doi.org/10.1016/j.gca.2012.04.003

Cannat, M., Sauter, D., Mendel, V. et al. (2006). Modes of seafloor generation at a melt-poor ultraslow-spreading ridge. *Geology 34* (7): 605–608. https://doi.org/10.1130/G22486.1

Cannat, M., Sauter, D., Bezos, A. et al. (2008). Spreading rate, spreading obliquity and melt supply at the ultraslow spreading Southwest Indian Ridge. *Geochemistry, Geophysics, Geosystems 9* (4): Q04002. https://doi.org/10.1029/2007GC001676

Cao, H., Wang, Y., Lee, O.O. et al. (2014). Microbial sulfur cycle in two hydrothermal chimneys on the Southwest Indian Ridge. *MBio 5* (1). https://doi.org/10.1128/mBio.00980-13

Cao, H., Sun, Z., Jiang, Z. et al. (2021). Source origin and ore-controlling factors of hydrothermal sulfides from the Tianzuo hydrothermal field, *Southwest Indian Ridge. Ore Geology Reviews 134*: 104168

Castelle, C.J., Wrighton, K.C., Thomas, B.C. et al. (2015). Genomic expansion of domain archaea highlights roles for organisms from new phyla in anaerobic carbon cycling. *Current Biology 25* (6): 690–701. https://doi.org/10.1016/j.cub.2015.01.014

Chan, C.S., Fakra, S.C., Emerson, D. et al. (2011). Lithotrophic iron-oxidizing bacteria produce organic stalks to control mineral growth: Implications for biosignature formation. *ISME Journal 5* (4): 717–727. https://doi.org/10.1038/ismej.2010.173

Chen, C., Copley, J.T., Linse, K. et al. (2015). The heart of a dragon: 3D anatomical reconstruction of the "scaly-foot gastropod" (Mollusca: Gastropoda: *Neomphalina*) reveals its extraordinary circulatory system. *Frontiers in Zoology 12* (1). https://doi.org/10.1186/s12983-015-0105-1

Chen, J., Tao, C., Liang, J. et al. (2018). Newly discovered hydrothermal fields along the ultraslow-spreading Southwest Indian Ridge around 63°E. *Acta Oceanologica Sinica 37* (11): 61–67. https://doi.org/10.1007/s13131-018-1333-y

Chinni, V., Singh, S.K., Bhushan, R. et al. (2019). Spatial variability in dissolved iron concentrations in the marginal and open waters of the Indian Ocean. *Marine Chemistry 208*: 11–28. https://doi.org/10.1016/j.marchem.2018.11.007

Cochran, J.R. and Sempéré, J.-C. (1997). The Southeast Indian Ridge between 88°E and 118°E: gravity anomalies and crustal accretion at intermediate spreading rates. *Journal of Geophysical Research: Solid Earth 102* (B7): 15463–15487. https://doi.org/10.1029/97jb00511

Copley, J.T., Marsh, L., Glover, A.G. et al. (2016). Ecology and biogeography of megafauna and macrofauna at the first known deep-sea hydrothermal vents on the ultraslow-spreading Southwest Indian Ridge. *Scientific Reports 6*. https://doi.org/10.1038/srep39158

Crépeau, V., Cambon Bonavita, M.A., Lesongeur, F. et al. (2011). Diversity and function in microbial mats from the Lucky Strike hydrothermal vent field. *FEMS Microbiology Ecology 76* (3): 524–540. https://doi.org/10.1111/j.1574-6941.2011.0107

de Angelis, M.A., Lilley, M.D., Olson, E.J. et al. (1993). Methane oxidation in deep-sea hydrothermal plumes of the Endeavor Segment of the Juan de Fuca Ridge. *Deep-Sea Res 40*: 1169–1186.

DeMets, C., Gordon, R.G., Argus, D.F. et al. (1994). Effect of recent revisions to the geomagnetic reversal time scale on estimates of current plate motions. *Geophysical Research Letters.* https://doi.org/10.1029/94GL02118

DeMets, C., Gordon, R.G. and Argus, D.F. (2010). Geologically current plate motions. *Geophysical Journal International 181* (1): 1–80. https://doi.org/10.1111/j.1365-246X.2009.0449

Dick, G.J., Clement, B.G., Webb, S.M. et al. (2009). Enzymatic microbial Mn (II) oxidation and Mn biooxide production in the Guaymas Basin deep-sea hydrothermal plume. *Geochimica et Cosmochimica Acta 73* (21): 6517–6530. https://doi.org/10.1016/j.gca.2009.07.039

Dick, G.J., Anantharaman, K., Baker, B.J. et al. (2013). The microbiology of deep-sea hydrothermal vent plumes: Ecological and biogeographic linkages to seafloor and water column habitats. *Frontiers in Microbiology.* https://doi.org/10.3389/fmicb.2013.00124

Dick, H.J.B., Lin, J. and Schouten, H. (2003). An ultraslow-spreading class of ocean ridge. *Nature 426* (6965): 405–412. https://doi.org/10.1038/nature02128

Ding, J., Zhang, Y., Wang, H. et al. (2017). Microbial community structure of deep-sea hydrothermal vents on the ultraslow spreading southwest Indian ridge. *Frontiers in Microbiology.* https://doi.org/10.3389/fmicb.2017.01012

Djurhuus, A., Mikalsen, S.O., Giebel, H.A. et al. (2017). Cutting through the smoke: The diversity of microorganisms in deep-sea hydrothermal plumes. *Royal Society Open Science 4* (4). https://doi.org/10.1098/rsos.160829

Elshahed, M.S., Youssef, N.H., Luo, Q. et al. (2007). Phylogenetic and metabolic diversity of Planctomycetes from anaerobic, sulfide- and sulfur-rich Zodletone Spring, Oklahoma. *Applied and Environmental Microbiology 73* (15): 4707–4716. https://doi.org/10.1128/AEM.00591-07

Emerson, D., Rentz, J.A., Lilburn, T.G. et al. (2007). A novel lineage of proteobacteria involved in formation of marine Fe-oxidizing microbial mat communities. *PLoS ONE 2* (8). https://doi.org/10.1371/journal. pone.0000667

Fagervold, S.K., Galand, P.E., Zbinden, M. et al. (2012). Sunken woods on the ocean floor provide diverse specialized habitats for microorganisms. *FEMS Microbiology Ecology 82* (3): 616–628. https://doi.org/10.1111/j.1574-6941.2012.0143

Fang, Z. and Wang, W.X. (2021). Size speciation of dissolved trace metals in hydrothermal plumes on the Southwest Indian Ridge. *Science of the Total Environment 771*: 145367

Fernandes, S.O., Krishnan, K.P., Khedekar, V.D. et al. (2005). Manganese oxidation by bacterial isolates from the Indian Ridge System. *BioMetals 18* (5): 483–492. https://doi.org/10.1007/s10534-005-3000-y

Fernandes, S.O., Surya Prakash, L., Balan Binish, M. et al. (2018). Changes in morphology and metabolism enable Mn-oxidizing bacteria from mid-oceanic ridge environment to counter metal-induced stress. *Journal of Basic Microbiology 58* (5): 390–402. https://doi.org/10.1002/jobm.201700580

Fisher, C.R., Takai, K. and le Bris, N. (2007). Hydrothermal vent ecosystems. *Oceanography 20* (1): 14–23. https://doi.org/10.5670/oceanog.2007.75

Fujii, M., Okino, K., Sato, T. et al. (2016). Origin of magnetic highs at ultramafic hosted hydrothermal systems: Insights from the Yokoniwa site of Central Indian Ridge. *Earth and Planetary Science Letters 441*: 26–37.

Füri, E., Hilton, D.R., Murton, B.J. et al. (2011). Helium isotope variations between Réunion Island and the Central Indian Ridge (17°–21°S): New evidence for ridge-hot spot interaction. *Journal of Geophysical Research: Solid Earth 116* (2): 1–17. https://doi.org/10.1029/2010JB007609

Gallant, R.M. and Von Damm, K.L. (2006). Geochemical controls on hydrothermal fluids from the kairei and edmond vent fields, 23°–25°S, Central Indian Ridge. *Geochemistry, Geophysics, Geosystems 7* (6). https://doi.org/10.1029/2005GC001067

Gamo, T., Nakayama, E., Shitashima, K. et al. (1996). Hydrothermal plumes at the Rodriguez triple junction, Indian ridge. *Earth and Planetary Science Letters 142* (1–2): 261–270. https://doi.org/10.1016/0012-821x (96)00087-8

Gamo, T., Chiba, H., Yamanaka, T. et al. (2001). Chemical characteristics of newly discovered black smoker fluids and associated hydrothermal plumes at the Rodriguez Triple Junction, Central Indian Ridge. *Earth and Planetary Science Letters 193* (3–4): 371–379. https://doi.org/10.1016/S0012-821X (01)00511-8

German, C.R. and Von Damm, K.L. (2003). Hydrothermal Processes. In: *Treatise on Geochemistry*, Vol. 6–9 (eds. H.D.

Holland and K.K. Turekian), pp. 181–222. Elsevier. https://doi.org/10.1016/B0-08-043751-6/06109-0

German, C.R., Campbell, A.C. and Edmond, J.M. (1991). Hydrothermal scavenging at the Mid-Atlantic Ridge: Modification of trace element dissolved fluxes. *Earth and Planetary Science Letters 107* (1): 101–114. https://doi.org/10.1016/0012-821X (91)90047-L

German, C.R., Baker, E.T., Mevel, C. et al. (1998). Hydrothermal activity along the southwest Indian ridge. *Nature 395* (6701): 490–493.

Gorlas, A., Jacquemot, P., Guigner, J.M. et al. (2018). Greigite nanocrystals produced by hyperthermophilic archaea of Thermococcales order. *PLoS ONE 13* (8). https://doi.org/10.1371/journal. pone.0201549

Götz, D., Banta, A., Beveridge, T.J. et al. (2002). *Persephonella marina* gen. nov., sp. nov. and *Persephonella guaymasensis* sp. nov., two novel, thermophilic, hydrogen-oxidizing microaerophiles from deep-sea hydrothermal vents. *International Journal of Systematic and Evolutionary Microbiology 52* (4): 1349–1359. https://doi.org/10.1099/ijs.0.02126-0

Halbach, P., Blum, N., Plüger, W. et al. (1995). The Sonne Field – first massive sulfides in the Indian Ocean. *InterRidge News 4* (2): 12–15

Haalboom, S., Price, D., Mienis, F. et al. (2019). Successional patterns of (trace) metals and microorganisms in the Rainbow hydrothermal vent plume at the Mid-Atlantic Ridge. *Biogeosciences Discussions 1–44*. https://doi.org/10.5194/bg-2019-189

Hallberg, K.B., Hedrich, S. and Johnson, D.B. (2011). *Acidiferrobacter thiooxydans*, gen. nov. sp. nov.; an acidophilic, thermo-tolerant, facultatively anaerobic iron- and sulfur-oxidizer of the family Ectothiorhodospiraceae. *Extremophiles 15* (2): 271–279. https://doi.org/10.1007/s00792-011-0359-2

Han, X., Wu, G., Cui, R. et al (2010) Discovery of a hydrothermal sulfide deposit on the Southwest Indian Ridge at 49.2_E. In: *American Geophysical Union, Fall Meeting 2010*, Abstract OS21C–1531

Han, Y., Gonnella, G., Adam, N. et al. (2018). Hydrothermal chimneys host habitat-specific microbial communities: analogues for studying the possible impact of mining seafloor massive sulfide deposits. *Scientific Reports 8* (1). https://doi.org/10.1038/s41598-018-28613-5

Hashimoto, J., Ohta, S., Gamo, T. et al. (2001). First hydrothermal vent communities from the Indian Ocean discovered. *Zoological Science 18* (5): 717–721. https://doi.org/10.2108/zsj.18.717

Haymon, R.M., Fornari, D.J., Von Damm, K.L. et al. (1993). Volcanic eruption of the mid-ocean ridge along the East Pacific Rise crest at 9°45–52′N: Direct submersible observations of seafloor phenomena associated with an eruption event in April, 1991. *Earth and Planetary Science Letters 119* (1–2): 85–101. https://doi.org/10.1016/0012-821X (93)90008-W

Hekinian R. (1982). *Petrology of the Ocean Floor. Elsevier Oceanography Series, 33*. Amsterdam: Elsevier.

Helfrich K.R. and Speer K.G. (1995) Ocean hydrothermal circulation: mesoscale and basin-scale flow. *Geophysical Monographs (AGU) 91*: 347–356.

Herrera, S., Watanabe, H. and Shank, T.M. (2015). Evolutionary and biogeographical patterns of barnacles from deep-sea hydrothermal vents. *Molecular Ecology 24* (3): 673–689. https://doi.org/10.1111/mec.13054

Herring, P.J. and Dixon, D.R. (1998). Extensive deep-sea dispersal of postlarval shrimp from a hydrothermal vent. *Deep-Sea Research Part I: Oceanographic Research Papers 45* (12): 2105–2118. https://doi.org/10.1016/S0967-0637 (98)00050-8

Hoehler, T.M., Alperin, M.J., Albert, D.B. et al. (1998). Thermodynamic control on hydrogen concentrations in anoxic sediments. *Geochimica et Cosmochimica Acta 62* (10): 1745–1756. https://doi.org/10.1016/S0016-7037 (98)00106-9

Hoek, J., Banta, A., Hubler, F. et al. (2003). Microbial diversity of a sulphide spire located in the Edmond deep-sea hydrothermal vent field on the Central Indian Ridge. *Geobiology 1* (2): 119–127. https://doi.org/10.1046/j.1472-4669.2003.0001

Huber, J.A., Cantin, H.V., Huse, S.M. et al. (2010). Isolated communities of *Epsilonproteobacteria* in hydrothermal vent fluids of the Mariana Arc seamounts. *FEMS Microbiology Ecology 73* (3): 538–549. https://doi.org/10.1111/j.1574-6941.2010.0091

Hügler, M., Wirsen, C.O., Fuchs, G. et al. (2005). Evidence for autotrophic CO2 fixation via the reductive tricarboxylic acid cycle by members of the ε subdivision of proteobacteria. *Journal of Bacteriology 187* (9): 3020–3027. https://doi.org/10.1128/JB.187.9.3020-3027.2005

Inagaki, F., Takai, K., Kobayashi, H. et al. (2003). *Sulfurimonas autrotrophica* gen. nov., sp. nov., a novel sulfur-oxidizing E-proteobacterium isolated from hydrothermal sediments in the Mid-Okinawa Trough. *International Journal of Systematic and Evolutionary Microbiology 53* (6): 1801–1805. https://doi.org/10.1099/ijs.0.02682-0

Jang, S.J., Ho, P.T., Jun, S.Y. et al. (2020). A newly discovered *Gigantidas* bivalve mussel from the Onnuri Vent Field in the northern Central Indian Ridge. *Deep-Sea Research Part I: Oceanographic Research Papers 161*: 103299. https://doi.org/10.1016/j.dsr.2020.103299

Jean-Baptiste, P., Mantisi, F., Pauwells, H. et al. (1992). Hydrothermal 3He and manganese plumes at 19°29′S on the Central Indian Ridge. *Geophysical Research Letters 19* (17): 1787–1790. https://doi.org/10.1029/92GL00577

Ji, F., Zhou, H., Yang, Q. et al. (2017). Geochemistry of hydrothermal vent fluids and its implications for subsurface processes at the active Longqi hydrothermal field, Southwest Indian Ridge. *Deep-Sea Research Part I: Oceanographic Research Papers 122*: 41–47. https://doi.org/10.1016/j.dsr.2017.02.001

Johnson, S.B., Warén, A., Tunnicliffe, V. et al. (2015). Molecular taxonomy and naming of five cryptic species of *Alviniconcha* snails (Gastropoda: Abyssochrysoidea) from hydrothermal vents. *Systematics and Biodiversity13* (3): 278–295. https://doi.org/10.1080/14772000.2014.970673

Juniper, S.K., Bird, D.F., Summit, M. et al. (1998). Bacterial and viral abundances in hydrothermal event plumes over northern Gorda Ridge. *Deep-Sea Research Part II: Topical Studies in Oceanography 45* (12): 2739–2749. https://doi.org/10.1016/S0967-0645 (98)00091-5

Kalangutkar, N.G., Iyer, S.D., Mascarenhas-Pereira, M.B.L. et al. (2015). Hydrothermal signature in ferromanganese oxide coatings on pumice from the Central Indian Ocean Basin. *Geo-Marine Letters 35* (3): 221–235. https://doi.org/10.1007/s00367-015-0402-x

Kamesh Raju, K.A., Ramprasad, T. and Subrahmanyam, C. (1997). Geophysical investigations over a segment of the

Central Indian Ridge, *Indian Ocean. Geo-Marine Letters 17* (3): 195–201. https://doi.org/10.1007/s003670050026

Kamesh Raju, K.A., Chaubey, A.K., Amarnath, D. et al. (2008). Morphotectonics of the Carlsberg Ridge between 62°20′ and 66°20′E, northwest Indian Ocean. *Marine Geology 252* (3–4): 120–128. https://doi.org/10.1016/j.margeo.2008.03.016

Kamesh Raju, K.A., Ray, D., Mudholkar, A. et al. (2012a). Tectonic and volcanic implications of a cratered seamount off Nicobar Island andaman Sea. *Journal of Asian Earth Sciences 56*: 42–53. https://doi.org/10.1016/j.jseaes.2012.04.018

Kamesh Raju, K.A., Samudrala, K., Drolia, R.K. et al. (2012b). Segmentation and morphology of the Central Indian Ridge between 3°S and 11°S, Indian Ocean. *Tectonophysics 554–557*: 114–126. https://doi.org/10.1016/j.tecto.2012.06.001

Kato, S., Kobayashi, C., Kakegawa, T. et al. (2009). Microbial communities in iron-silica-rich microbial mats at deep-sea hydrothermal fields of the Southern Mariana Trough. *Environmental Microbiology 11* (8): 2094–2111. https://doi.org/10.1111/j.1462-2920.2009.0193

Kawagucci, S., Miyazaki, J., Noguchi, T. et al. (2016). Fluid chemistry in the Solitaire and Dodo hydrothermal fields of the Central Indian Ridge. *Geofluids 16* (5): 988–1005. https://doi.org/10.1111/gfl.12201

Kawagucci, Shinsuke, Okamura, K. et al. (2008). Methane, manganese and helium-3 in newly discovered hydrothermal plumes over the Central Indian Ridge, 18°–20°S. *Geochemistry, Geophysics, Geosystems 9* (10). https://doi.org/10.1029/2008GC002082

Kim, J., Son, S.K., Kim, D. et al. (2020). Discovery of active hydrothermal vent fields along the Central Indian Ridge, 8–12°S. *Geochemistry, Geophysics, Geosystems 21* (8): 0–3. https://doi.org/10.1029/2020GC009058

Kleiveland, C.R., Hult, L.T.O., Kuczkowska, K. et al. (2012). Draft genome sequence of the methane-oxidizing bacterium *Methylococcus capsulatus* (Texas). *Journal of Bacteriology 194* (23).. https://doi.org/10.1128/JB.01656-12

Kuhn, T., Bau, M., Blum, N. and Halbach, P. (1998). Origin of negative Ce anomalies in mixed hydrothermal-hydrogenetic Fe-Mn crusts from the Central Indian Ridge. *Earth and Planetary Science Letters 163* (1–4): 207–220. https://doi.org/10.1016/S0012-821X (98)00188-5

Kuhn, T., Burger, H., Castradori, D. et al. (2000). Volcanic and hydrothermal history of ridge segments near the Rodrigues Triple Junction (Central Indian Ocean) deduced from sediment geochemistry. *Marine Geology 169* (3–4): 391–409. https://doi.org/10.1016/S0025-3227 (00)00080-3

Kumagai, H., Nakamura, K., Toki, T. et al. (2008). Geological background of the Kairei and Edmond hydrothermal fields along the Central Indian Ridge: Implications of their vent fluids'distinct chemistry. In: *Geofluids* (Vol. *8*, pp. 239–251). https://doi.org/10.1111/j.1468-8123.2008.0022

Kumar, M.D. and Li, Y.H. (1996). Spreading of water masses and regeneration of silica and 226Ra in the Indian Ocean. *Deep-Sea Research Part II: Topical Studies in Oceanography 43* (1): 83–110. https://doi.org/10.1016/0967-0645 (95)00084-4

Kurian, S., Nath, B.N., Ramaswamy, V. et al. (2008). Possible detrital, diagenetic and hydrothermal sources for Holocene sediments of the Andaman backarc basin. *Marine Geology 247* (3–4): 178–193. https://doi.org/10.1016/j.margeo.2007.09.006

L'Haridon, S., Reysenbach, A.L., Banta, A. et al. (2003). *Methanocaldococcus indicus* sp. nov., a novel hyperthermophilic methanogen isolated from the Central Indian Ridge. *International Journal of Systematic and Evolutionary Microbiology 53* (6): 1931–1935. https://doi.org/10.1099/ijs.0.02700-0

La Duc, M.T., Benardini, J.N., Kempf, M.J. et al. (2007). Microbial diversity of Indian ocean hydrothermal vent plumes: microbes tolerant of desiccation. Peroxide exposure and ultraviolet and γ-irradiation. *Astrobiology 7*: 416–431. doi:10.1089/ast.2006.0060

Labrenz, M., Grote, J., Mammitzsch, K. et al. (2013). *Sulfurimonas gotlandica* sp. nov., a chemoautotrophic and psychrotolerant epsilonproteobacterium isolated from a pelagic redoxcline and an emended description of the genus *Sulfurimonas*. *International Journal of Systematic and Evolutionary Microbiology 63* (11): 4141–4148. https://doi.org/10.1099/ijs.0.048827-0

Lalou, C., Münch, U., Halbach, P. and Reyss, J.L. (1998). Radiochronological investigation of hydrothermal deposits from the MESO zone, *Central Indian Ridge. Marine Geology 149* (1–4): 243–254

Lam, P., Cowen, J.P. and Jones, R.D. (2004). Autotrophic ammonia oxidation in a deep-sea hydrothermal plume. *FEMS Microbiology Ecology 47* (2): 191–206. https://doi.org/10.1016/S0168-6496 (03)00256-3

Lam, P., Cowen, J.P., Popp, B.N. and Jones, R.D. (2008). Microbial ammonia oxidation and enhanced nitrogen cycling in the Endeavour hydrothermal plume. *Geochimica et Cosmochimica Acta 72* (9): 2268–2286. https://doi.org/10.1016/j.gca.2008.01.033

Lang, S.Q. (2018). Hydrothermal stamp on the oceans. *Nature Geoscience 11* (1): 10–12. https://doi.org/10.1038/s41561-017-0044-x

Le Bris N., Arnaud-Haond S., Beaulieu S. et al. (2016). Hydrothermal vents and cold seeps. In: *First Global Integrated Marine Assessment* (ed. United Nations), 853–862. Cambridge University Press.

Lecoeuvre A, Menez B, Lecourt L. et al. (2018). Microbial ecology linked to serpentinization processes and related carbonation at the Old City hydrothermal field. *Goldschmidt Abstracts 2018*: 1428.

Lecoeuvre, A., Ménez, B., Cannat, M. et al. (2021). Microbial ecology of the newly discovered serpentinite-hosted Old City hydrothermal field (southwest Indian ridge). *The ISME Journal 15*: 818–832. https://doi.org/10.1038/s41396-020-00816-7

Lei, J., Chu, F., Yu, X. et al. (2017). Lipid biomarkers reveal microbial communities in hydrothermal chimney structures from the 49.6°E Hydrothermal Vent Field at the Southwest Indian Ocean Ridge. *Geomicrobiology Journal 34* (6): 557–566. https://doi.org/10.1080/01490451.2016.1238979

Levin, L.A. and Sibuet, M. (2012). Understanding continental margin biodiversity: a new imperative. *Annual Review of Marine Science 4* (1): 79–112. https://doi.org/10.1146/annurev-marine-120709-142714

Li, J., Zhou, H., Fang, J., Wu, Z. et al. (2016). Microbial distribution in a hydrothermal plume of the Southwest Indian Ridge. *Geomicrobiology Journal 33* (5): 401–415. https://doi.org/10.1080/01490451.2015.1048393

Li, J., Cui, J., Yang, Q. et al. (2017). Oxidative weathering and microbial diversity of an inactive seafloor hydrothermal sulfide chimney. *Frontiers in Microbiology 8*. https://doi.org/10.3389/fmicb.2017.01378

Li, M., Toner, B.M., Baker, B.J. et al. (2014). Microbial iron uptake as a mechanism for dispersing iron from deep-sea hydrothermal vents. *Nature Communications 5*. https://doi.org/10.1038/ncomms4192

Li, M., Baker, B.J., Anantharaman, K. et al. (2015). Genomic and transcriptomic evidence for scavenging of diverse organic compounds by widespread deep-sea archaea. *Nature Communications 6*. https://doi.org/10.1038/ncomms9933

Liao, S., Tao, C., Li, H. et al. (2018). Surface sediment geochemistry and hydrothermal activity indicators in the Dragon Horn area on the Southwest Indian Ridge. *Marine Geology 398*: 22–34. https://doi.org/10.1016/j.margeo.2017.12.005

Liao, S., Tao, C., Dias, Á.A. et al. (2019). Surface sediment composition and distribution of hydrothermal derived elements at the Duanqiao-1 hydrothermal field, *Southwest Indian Ridge. Marine Geology 416*: 105975.

Lim, J.K., Kim, Y.J., Yang, JA. et al. (2020). *Thermococcus indicus* sp. nov., a Fe (III)-reducing hyperthermophilic archaeon isolated from the Onnuri Vent Field of the Central Indian Ocean ridge. *Journal of Microbiology 58* 260–267. https://doi.org/10.1007/s12275-020-9424-9

Lin, T.J., Ver Eecke, H.C., Breves, E.A. et al. (2016). Linkages between mineralogy, fluid chemistry and microbial communities within hydrothermal chimneys from the Endeavour Segment, Juan de Fuca Ridge. *Geochemistry, Geophysics, Geosystems 17* (2): 300–323. https://doi.org/10.1002/2015GC006091

Manzella, M.P., Holmes, D.E., Rocheleau, J.M. et al. (2015). The complete genome sequence and emendation of the hyperthermophilic, obligate iron-reducing archaeon "*Geoglobus ahangari*" strain 234T. *Standards in Genomic Sciences 10* (1). https://doi.org/10.1186/s40793-015-0035-8

Marshall, K.T. and Morris, R.M. (2013). Isolation of an aerobic sulfur oxidizer from the SUP05/Arctic96BD-19 clade. *ISME Journal 7* (2): 452–455. https://doi.org/10.1038/ismej.2012.78

Maruyama, A., Urabe, T., Ishibashi, J. et al. (1998). Global hydrothermal primary production rate estimated from the southern East Pacific Rise. *Cahiers de Biologie Marine 39* (3–4): 249–252. https://doi.org/10.21411/cbm. a.ec0e1360

Mascarenhas-Pereira, M.B.L. and Nath, B.N. (2010). Selective leaching studies of sediments from a seamount flank in the Central Indian Basin: Resolving hydrothermal, volcanogenic and terrigenous sources using major, trace and rare-earth elements. *Marine Chemistry 121* (1–4): 49–66. https://doi.org/10.1016/j.marchem.2010.03.004

Mazumdar, A., Dewangan, P., Joäo, H.M. et al. (2009). Evidence of paleo-cold seep activity from the Bay of Bengal, offshore India. *Geochemistry, Geophysics, Geosystems 10* (6). https://doi.org/10.1029/2008GC002337

Mazumdar, A., Dewangan, P., Peketi, A. et al. (2019). The first record of active methane (cold) seep ecosystem associated with shallow methane hydrate from the Indian EEZ. *Journal of Earth System Science 128*: 18. https://doi.org/10.1007/s12040-018-1044-y

McCollom, T.M. (2008). Observational, experimental and theoretical constraints on carbon cycling in mid-ocean ridge hydrothermal systems. In: *Magma to Microbe: Modeling Hydrothermal Processes at Ocean Spreading Centers*, (eds. R.P. Lowell, J.S. Seewald, A. Metaxas et al.), 193–213. AGU.

Mendel, V. and Sauter, D. (1997). Seamount volcanism at the super slow-spreading Southwest Indian Ridge between 57°E and 70°E. *Geology 25* (2): 299–102. https://doi.org/10.1130/0091-7613 (1997)025<0099:SVATSS>2.O;2

Mendel, V., Sauter, D., Parson, L. et al. (1997). Segmentation and morphotectonic variations along a super slow-spreading center: the Southwest Indian Ridge (57°E–70° E). *Marine Geophysical Research.* https://doi.org/10.1023/A:1004232506333

Miller, A.J., Fan, X., Orsel, M. et al. (2007). Nitrate transport and signalling. *Journal of Experimental Botany 58*: 2297–2306). https://doi.org/10.1093/jxb/erm066

Mino, S., Makita, H., Toki, T. et al. (2013). Biogeography of *Persephonella* in deep-sea hydrothermal vents of the Western Pacific. *Frontiers in Microbiology 4*. https://doi.org/10.3389/fmicb.2013.00107

Mino, S., Nakagawa, S., Makita, H. et al. (2017). Endemicity of the cosmopolitan mesophilic chemolithoautotroph Sulfurimonas at deep-sea hydrothermal vents. *ISME Journal 11* (4): 909–919. https://doi.org/10.1038/ismej.2016.178

Moussard, H., L'Haridon, S., Tindall, B.J. et al. (2004). *Thermodesulfatator indicus* gen. nov., sp. nov., a novel thermophilic chemolithoautotrophic sulfate-reducing bacterium isolated from the Central Indian Ridge. *International Journal of Systematic and Evolutionary Microbiology 54* (1): 227–233. https://doi.org/10.1099/ijs.0.02669-0

Münch, U., Blum, N. and Halbach, P. (1999). Mineralogical and geochemical features of sulfide chimneys from the MESO zone, Central Indian Ridge. *Chemical Geology 155* (1–2): 29–44

Munch, U., Lalou, C., Halbach, P. et al. (2001). Relict hydrothermal events along the super-slow Southwest Indian spreading ridge near 63856 X E-mineralogy, chemistry and chronology of sulfide samples. *Chemical Geology 177*: 341–349.

Mullineaux, L.S., Metaxas, A., Beaulieu, S.E. et al. (2018). Exploring the ecology of deep-sea hydrothermal vents in a metacommunity framework. *Frontiers in Marine Science.* https://doi.org/10.3389/fmars.2018.00049

Murton, B.J., Baker, E.T., Sands, C.M. et al. (2006). Detection of an unusually large hydrothermal event plume above the slow-spreading Carlsberg Ridge: NW Indian Ocean. *Geophysical Research Letters 33* (10). https://doi.org/10.1029/2006GL026048

Naganuma, T., Otsuki, A. and Seki, H. (1989). Abundance and growth rate of bacterioplankton community in hydrothermal vent plumes of the North Fiji Basin. *Deep Sea Research Part A, Oceanographic Research Papers 36* (9): 1379–1390. https://doi.org/10.1016/0198-0149 (89)90089-7

Nakagawa, S. and Takai, K. (2008). Deep-sea vent chemoautotrophs: diversity, biochemistry and ecological significance. *FEMS Microbiology Ecology.* https://doi.org/10.1111/j.1574-6941.2008.0050

Nakagawa, T., Nakagawa, S., Inagaki, F. et al. (2004). Phylogenetic diversity of sulfate-reducing prokaryotes in active deep-sea hydrothermal vent chimney structures. *FEMS Microbiology Letters 232* (2): 145–152. https://doi.org/10.1016/S0378-1097 (04)00044-8

Nakamura, K. and Takai, K. (2015a). Geochemical constraints on potential biomass sustained by subseafloor water–rock interactions. In: *Subseafloor Biosphere Linked to Hydrothermal Systems: TAIGA Concept* (eds. J. Ishibashi, K. Okino, M. Sunamura), 11–30. Springer. https://doi.org/10.1007/978-4-431-54865-2_2

Nakamura, K. and Takai, K. (2015b). Indian Ocean hydrothermal systems: Seafloor hydrothermal activities, physical and chemical characteristics of hydrothermal fluids and vent-associated biological communities. In: *Subseafloor Biosphere Linked to Hydrothermal Systems: TAIGA Concept* (eds. J. Ishibashi, K. Okino and M. Sunamura), 147–161. Springer. https://doi.org/10.1007/978-4-431-54865-2_12

Nakamura, K., Morishita, T., Bach, W. et al. (2009). Serpentinized troctolites exposed near the Kairei Hydrothermal Field, Central Indian Ridge: insights into the origin of the Kairei hydrothermal fluid supporting a unique microbial ecosystem. *Earth and Planetary Science Letters 280* (1–4): 128–136. https://doi.org/10.1016/j.epsl.2009.01.024

Nakamura, K., Watanabe, H., Miyazaki, J. et al. (2012). Discovery of new hydrothermal activity and chemosynthetic fauna on the Central Indian ridge at 18°–20°S. *PLoS ONE 7* (3). https://doi.org/10.1371/journal. pone.0032965

Nakamura, K., Toki, T., Mochizuki, N. et al. (2013). Discovery of a new hydrothermal vent based on an underwater, high-resolution geophysical survey. *Deep-Sea Research Part I: Oceanographic Research Papers 74*: 1–10. https://doi.org/10.1016/j.dsr.2012.12.003

Nath, B.N., Balaram, V., Sudhakar, M. et al. (1992). Rare earth element geochemistry of ferromanganese deposits from the Indian Ocean. *Marine Chemistry 38* (3–4): 185–208. https://doi.org/10.1016/0304-4203 (92)90034-8

Nath, B.N., Plüger, W.L. and Roelandts, I. (1997). Geochemical constraints on the hydrothermal origin of ferromanganese encrustations from the Rodriguez Triple Junction, Indian Ocean. *Geological Society Special Publication 119*: 199–211. https://doi.org/10.1144/GSL. SP.1997.119.01.13

Nayak, B., Halbach, P., Pracejus, B. et al. (2014). Massive sulfides of Mount Jourdanne along the super-slow spreading Southwest Indian Ridge and their genesis. *Ore Geology Reviews 63*: 115–128.

Nishioka, J., Obata, H. and Tsumune, D. (2013). Evidence of an extensive spread of hydrothermal dissolved iron in the Indian Ocean. *Earth and Planetary Science Letters 361*: 26–33. https://doi.org/10.1016/j.epsl.2012.11.040

Nobu, M.K., Narihiro, T., Kuroda, K. et al. (2016). Chasing the elusive Euryarchaeota class WSA2: Genomes reveal a uniquely fastidious methyl-reducing methanogen. *ISME Journal 10* (10): 2478–2487. https://doi.org/10.1038/ismej.2016.33

Noguchi, T., Fukuba, T., Okamura, K. et al. (2015). Distribution and biogeochemical properties of hydrothermal plumes in the Rodriguez triple junction. In: *Subseafloor Biosphere Linked to Hydrothermal Systems: TAIGA Concept* (eds. J. Ishibashi, K. Okino and M. Sunamura), 195–204. Springer. https://doi.org/10.1007/978-4-431-54865-2_15

Noowong, A., Gomez-Saez, G.V., Hansen, C.T. et al. (2021). Imprint of Kairei and Pelagia deep-sea hydrothermal systems (Indian Ocean) on marine dissolved organic matter. *Organic Geochemistry 152*: 104141

Okino, K., Nakamura, K. and Sato, H. (2015). Tectonic background of four hydrothermal fields along the central Indian ridge. In: *Subseafloor Biosphere Linked to Hydrothermal Systems: TAIGA Concept* (eds. J. Ishibashi, K. Okino and M. Sunamura), 133–146. Springer. https://doi.org/10.1007/978-4-431-54865-2_11

Patriat, P. and Segoufin, J. (1988). Reconstruction of the Central Indian Ocean. *Tectonophysics 155* (1–4): 211–234. https://doi.org/10.1016/0040-1951 (88)90267-3

Patwardhan, S., Foustoukos, D.I., Giovannelli, D. et al. (2018). Ecological succession of sulfur-oxidizing epsilon- and gammaproteobacteria during colonization of a shallow-water gas vent. *Frontiers in Microbiology 9* (DEC). https://doi.org/10.3389/fmicb.2018.02970

Peng, X., Chen, S., Zhou, H. et al. (2011). Diversity of biogenic minerals in low-temperature Si-rich deposits from a newly discovered hydrothermal field on the ultraslow spreading Southwest Indian Ridge. *Journal of Geophysical Research: Biogeosciences 116* (3). https://doi.org/10.1029/2011JG001691

Peng, X.T., Zhou, H.Y., Yao, H.Q. et al. (2007). Microbe-related precipitation of iron and silica in the Edmond deep-sea hydrothermal vent field on the Central Indian Ridge. *Chinese Science Bulletin 52* (23): 3233–3238. https://doi.org/10.1007/s11434-007-0523-3

Pester, M., Schleper, C. and Wagner, M. (2011). The Thaumarchaeota: an emerging view of their phylogeny and ecophysiology. *Current Opinion in Microbiology 14* (3): 300–306. https://doi.org/10.1016/j.mib.2011.04.007

Piotrowski, A.M., Banakar, V.K., Scrivner, A.E. et al. (2009). Indian Ocean circulation and productivity during the last glacial cycle. *Earth and Planetary Science Letters 285* (1–2): 179–189. https://doi.org/10.1016/j.epsl.2009.06.007

Pjevac, P., Meier, D.V., Markert, S. et al. (2018). Metaproteogenomic profiling of microbial communities colonizing actively venting hydrothermal chimneys. *Frontiers in Microbiology 9*. https://doi.org/10.3389/fmicb.2018.00680

Pluger, W.L. (1990). Discovery of hydrothermal fields at the Central Indian Ridge. *Marine Mining 9* (1).

Popoola, S.O., Han, X., Wang, Y. et al. (2019a). Geochemical investigations of Fe-Si-Mn oxyhydroxides deposits in Wocan hydrothermal field on the slow-spreading Carlsberg ridge, Indian ocean: constraints on their types and origin. *Minerals 9* (1). https://doi.org/10.3390/min9010019

Popoola, S.O., Han, X., Wang, Y. et al. (2019b). Mineralogical and geochemical signatures of metalliferous sediments in wocan-1 and wocan-2 hydrothermal sites on the Carlsberg Ridge, Indian Ocean. *Minerals 9* (1). https://doi.org/10.3390/min9010026

Rao, P.S., Kamesh Raju, K.A., Ramprasad, T. et al. (1996). Evidence for hydrothermal activity in the Andaman Backarc Basin. *Current Science 70*, 379–384.

Ray, D., Mirza, I.H., Surya Prakash, L. et al. (2008). Water-column geochemical anomalies associated with the remnants of a mega plume: a case study after CR-2003 hydrothermal event in Carlsberg Ridge, *NW Indian Ocean. Current Science*, *95* (3): 355–360.

Ray, D., Kamesh Raju, K.A., Baker, E.T. et al. (2012). Hydrothermal plumes over the Carlsberg Ridge, Indian Ocean. *Geochemistry, Geophysics, Geosystems 13* (1): Q01009. https://doi.org/10.1029/2011GC003888

Ray, D., Babu, E.V.S.S.K. and Prakash, L.S. (2017). Nature of suspended particles in hydrothermal plume at 3°40'N Carlsberg Ridge: A comparison with deep oceanic suspended matter. *Current Science 112* (1): 139–146. https://doi.org/10.18520/cs/v112/i01/139-146

Ray, D., KameshRaju, K.A., Srinivas Rao, A. et al. (2020). Elevated turbidity and dissolved manganese in deep water column near 10°47'S Central Indian Ridge: studies on hydrothermal activities. *Geo-Marine Letters 40*: 619–628. https://doi.org/10.1007/s00367-020-00657-5

Reysenbach, A.L., Banta, A.B., Boone, D.R. et al. (2000). Microbial essentials at hydrothermal vents. *Nature 404* (6780): 835. https://doi.org/10.1038/35009029

Reysenbach, A.L., Götz, D., Banta, A. et al. (2002). Expanding the distribution of the Aquificales to the deep-sea vents on Mid-Atlantic Ridge and Central Indian Ridge. *Cahiers de Biologie Marine 43* (3–4): 425–428.

Reysenbach, A.L., Liu, Y., Banta, A.B. et al. (2006). A ubiquitous thermoacidophilic archaeon from deep-sea hydrothermal vents. *Nature 442* (7101): 444–447. https://doi.org/10.1038/nature04921

Royer, J.Y. and Sandwell, D.T. (1989). Evolution of the eastern Indian Ocean since the Late Cretaceous: constraints from Geosat altimetry. *Journal of Geophysical Research 94* (B10). https://doi.org/10.1029/jb094ib10p13755

Royer, J.Y., Patriat, P., Bergh, H.W. et al. (1988). Evolution of the Southwest Indian Ridge from the Late Cretaceous (anomaly 34) to the Middle Eocene (anomaly 20). *Tectonophysics 155* (1–4): 235–260. https://doi.org/10.1016/0040-1951 (88)90268-5

Ryu, T., Woo, S. and Lee, N. (2019). The first reference transcriptome assembly of the stalked barnacle, Neolepas marisindica, from the Onnuri Vent Field on the Central Indian Ridge. *Marine Genomics 48*. https://doi.org/10.1016/j.margen.2019.04.004

Sato, H., Nakamura, K., Kumagai, H. et al. (2015). Petrology and geochemistry of mid-ocean ridge basalts from the Southern Central Indian Ridge. In: *Subseafloor Biosphere Linked to Hydrothermal Systems: TAIGA Concept* (eds. J. Ishibashi, K. Okino, M. Sunamura), 163–175). Springer.

Sauter, D., Patriat, P., Rommevaux-Jestin, C. et al. (2001). The Southwest Indian Ridge between 49°15′E and 57°E: focused accretion and magma redistribution. *Earth and Planetary Science Letters 192* (3): 303–317. https://doi.org/10.1016/S0012-821X (01)00455-1

Sauter, D., Cannat, M., Roumejon, S. et al. (2013). Continuous exhumation of mantle-derived rocks at the southwest Indian Ridge for 11 million years. *Nature Geoscience 6*: 314–20.

Schrenk, M.O., Kelley, D.S., Delaney, J.R. et al. (2003). Incidence and diversity of microorganisms within the walls of an active deep-sea sulfide chimney. *Applied and Environmental Microbiology 69* (6): 3580–3592.

Sela-Adler, M., Ronen, Z., Herut, B. et al. (2017). Co-existence of methanogenesis and sulfate reduction with common substrates in sulfate-rich estuarine sediments. *Frontiers in Microbiology 8*. https://doi.org/10.3389/fmicb.2017.00766

Shah, V., Zhao, X., Lundeen, R.A. et al. (2019). Morphological plasticity in a sulfur-oxidizing marine bacterium from the SUP05 clade enhances dark carbon fixation. *MBio 10* (3). https://doi.org/10.1128/mBio.00216-19

Sievert, S.M., Scott, K.M., Klotz, M.G., Chain, P.S.G., Hauser, L.J., Hemp, J. et al. (2008). Genome of the epsilonproteobacterial chemolithoautotroph *Sulfurimonas denitrificans*. *Applied and Environmental Microbiology 74* (4): 1145–1156. https://doi.org/10.1128/AEM.01844-07

Sinha, R.K., Krishnan, K.P. and John Kurian, P. (2017). Draft genome sequence of Idiomarina sp. strain 5.13, a highly stress-resistant bacterium isolated from the Southwest Indian Ridge. *Genome Announcements 5* (10). https://doi.org/10.1128/genomeA.01747-16

Sinha, R.K., Krishnan, K.P., Thomas, F.A. et al. (2019). Polyphasic approach revealed complex bacterial community structure and function in deep sea sediment of ultra-slow spreading Southwest Indian Ridge. *Ecological Indicators 96*, 40–51. https://doi.org/10.1016/j.ecolind.2018.08.063

Sintes, E., Bergauer, K., De Corte, D. et al. (2013). Archaeal amoA gene diversity points to distinct biogeography of ammonia-oxidizing Crenarchaeota in the ocean. *Environmental Microbiology 15* (5): 1647–1658. https://doi.org/10.1111/j.1462-2920.2012.0280

Small, C., Cochran, J.R., Sempéré, J.C. et al. (1999). The structure and segmentation of the Southeast Indian Ridge. *Marine Geology 161* (1): 1–12. https://doi.org/10.1016/S0025-3227 (99)00051-1

Smith, G.J., Angle, J.C., Solden, L.M. et al. (2018). Members of the genus *Methylobacter* are inferred to account for the majority of aerobic methane oxidation in oxic soils from a freshwater wetland. *MBio 9* (6). https://doi.org/10.1128/mBio.00815-18

Son, J., Pak, S.J., Kim, J. et al. (2014). Tectonic and magmatic control of hydrothermal activity along the slow-spreading Central Indian Ridge, 8S-17S. *Geochemistry, Geophysics, Geosystems 15* (5): 2011–2020. https://doi.org/10.1002/2013GC005206

Srinivasan, A., Top, Z., Schlosser, P. et al. (2004). Mantle 3He distribution and deep circulation in the Indian Ocean. *Journal of Geophysical Research: Oceans 109* (C6).

Stokke, R., Dahle, H., Roalkvam, I. et al. (2015). Functional interactions among filamentous *Epsilonproteobacteria* and Bacteroidetes in a deep-sea hydrothermal vent biofilm. *Environmental Microbiology 17* (10): 4063–4077. https://doi.org/10.1111/1462-2920.12970

Sun, J., Zhou, Y., Chen, C. et al. (2020). Nearest vent, dearest friend: biodiversity of Tiancheng vent field reveals cross-ridge similarities in the Indian Ocean. *Royal Society Open Science 7* (3). https://doi.org/10.1098/rsos.200110

Surya Prakash, L., Ray, D., Paropkari, A.L. et al. (2012). Distribution of REEs and yttrium among major geochemical phases of marine Fe-Mn-oxides: Comparative study between hydrogenous and hydrothermal deposits. *Chemical Geology 312–313*: 127–137. https://doi.org/10.1016/j.chemgeo.2012.03.024

Surya Prakash, L., Ray, D., B.N.Nath., Satyanarayanan, M. et al. (2020). Anomalous phase association of REE in ferromanganese crusts from Indian mid-oceanic ridges: evidence for large scale dispersion of hydrothermal iron. *Chemical Geology 549*. https://doi.org/10.1016/j.chemgeo.2020.119679

Suzuki, Y., Inagaki, F., Takai, K. et al. (2004). Microbial diversity in inactive chimney structures from deep-sea hydrothermal systems. *Microbial Ecology 47*: 186–196). https://doi.org/10.1007/s00248-003-1014-y

Suzuki, Y., Sasaki, T., Suzuki, M. et al. (2005). Novel chemoautotrophic endosymbiosis between a member of the *Epsilonproteobacteria* and the hydrothermal-vent gastropod *Alviniconcha* aff. *hessleri* (Gastropoda: Provannidae) from the Indian Ocean. *Applied and Environmental Microbiology 71* (9): 5440–5450. https://doi.org/10.1128/AEM.71.9.5440-5450.2005

Sylvan, J.B., Sia, T.Y., Haddad, A.G. et al. (2013). Low temperature geomicrobiology follows host rock composition along a geochemical gradient in Lau Basin. *Frontiers in Microbiology 4*. https://doi.org/10.3389/fmicb.2013.00061

Takahata, N., Shirai, K., Ohmori, K. et al. (2018). Distribution of helium-3 plumes and deep-sea circulation in the central Indian Ocean. *Terrestrial, Atmospheric and Oceanic Sciences 29* (3): 331–340. https://doi.org/10.3319/TAO.2017.10.21.02

Takai, K. and Nakamura, K. (2010). Compositional, physiological and metabolic variability in microbial communities associated with geochemically diverse, deep-sea hydrothermal vent fluids. In: *Geomicrobiology: Molecular and Environmental Perspective*, 251–283. Springer. https://doi.org/10.1007/978-90-481-9204-5_12

Takai, K., Inagaki, F., Nakagawa, S. et al. (2003). Isolation and phylogenetic diversity of members of previously uncultivated ε-Proteobacteria in deep-sea hydrothermal fields. *FEMS Microbiology Letters 218* (1): 167–174. https://doi.org/10.1016/S0378-1097 (02)01147-3

Takai, K., Gamo, T., Tsunogai, U. et al. (2004). Geochemical and microbiological evidence for a hydrogen-based, hyperthermophilic subsurface lithoautotrophic microbial ecosystem (HyperSLiME) beneath an active deep-sea hydrothermal field. *Extremophiles 8* (4): 269–282. https://doi.org/10.1007/s00792-004-0386-3

Takai, K., Nealson, K.H. and Horikoshi, K. (2004a). Hydrogenimonas thermophila gen. nov., sp. nov., a novel thermophilic, hydrogen-oxidizing chemolithoautotroph within the E-Proteobacteria, isolated from a black smoker in a Central Indian Ridge hydrothermal field. *International Journal of Systematic and Evolutionary Microbiology 54* (1): 25–32. https://doi.org/10.1099/ijs.0.02787-0

Takai, K., Nealson, K.H. and Horikoshi, K. (2004b). *Methanotorris formicicus* sp. nov., a novel extremely thermophilic, methane-producing archaeon isolated from a black smoker chimney in the Central Indian Ridge. *International Journal of Systematic and Evolutionary Microbiology*, *54* (4): 1095–1100. https://doi.org/10.1099/ijs.0.02887-0

Takai, K., Nunoura, T., Ishibashi, J.I. et al. (2008). Variability in the microbial communities and hydrothermal fluid chemistry at the newly discovered Mariner hydrothermal field, southern Lau Basin. *Journal of Geophysical Research: Biogeosciences 113* (2). https://doi.org/10.1029/2007JG000636

Tao, C.H., Li, H.M., Huang, W. et al. (2011). Mineralogical and geochemical features of sulfide chimneys from the 49°39′E hydrothermal field on the Southwest Indian Ridge and their geological inferences. *Chinese Science Bulletin 56* (26): 2828–2838. https://doi.org/10.1007/s11434-011-4619-4

Tao, C., Lin, J., Guo, S. et al. (2012). First active hydrothermal vents on an ultraslow-spreading center: Southwest Indian Ridge. *Geology 40* (1): 47–50. https://doi.org/10.1130/G32389.1

Tao, C., Wu, G., Deng, X. et al. (2013). New discovery of seafloor hydrothermal activity on the Indian Ocean Carlsberg Ridge and Southern North Atlantic Ridge-progress during the 26th Chinese COMRA cruise. *Acta Oceanologica Sinica 32* (8): 85–88. https://doi.org/10.1007/s13131-013-0345-x

Tao, C., Li, H., Jin, X. et al. (2014). Seafloor hydrothermal activity and polymetallic sulfide exploration on the southwest Indian ridge. *Chinese Science Bulletin 59* (19): 2266–2276. https://doi.org/10.1007/s11434-014-0182-0

Tao, C., Seyfried, W.E., Lowell, R.P. et al. (2020). Deep high-temperature hydrothermal circulation in a detachment faulting system on the ultra-slow spreading ridge. *Nature communications 11* (1): 1–9

Topçuoglu, B.D., Stewart, L.C., Morrison, H.G. et al. (2016). Hydrogen limitation and syntrophic growth among natural assemblages of thermophilic methanogens at deep-sea hydrothermal vents. *Frontiers in Microbiology 7*. https://doi.org/10.3389/fmicb.2016.01240

Urabe, T., Ishibashi, J.I., Sunamura, M. et al. (2015). Interdisciplinary studies: introduction of TAIGA concept. In: *Subseafloor Biosphere Linked to Hydrothermal Systems: TAIGA Concept* (eds. J. Ishibashi, K. Okino and M. Sunamura), 1–10. Springer. https://doi.org/10.1007/978-4-431-54865-2_1

Van Dover, C.L. (2000). *The Ecology of Deep-Sea Hydrothermal Vents*. Princeton: Princeton University Press.

Van Dover, C.L., Humphris, S.E., Fornari, D. et al. (2001). Biogeography and ecological setting of Indian Ocean hydrothermal vents. *Science 294* (5543): 818–823. https://doi.org/10.1126/science.1064574

Van Dover, C.L., German, C.R., Speer, K.G. et al. (2002). Evolution and biogeography of deep-sea vent and seep invertebrates. *Science 295* (5558): 1253–1257. https://doi.org/10.1126/science.1067361

Vetriani, C., Speck, M.D., Ellor, S.V. et al. (2004). *Thermovibrio ammonificans* sp. nov., a thermophilic, chemolithotrophic, nitrate-ammonifying bacterium from deep-sea hydrothermal vents. *International Journal of Systematic and Evolutionary Microbiology 54* (1): 175–181. https://doi.org/10.1099/ijs.0.02781-0

Vlastélic, I., Abouchami, W., Galer, S.J.G. et al. (2001). Geographic control on Pb isotope distribution and sources in Indian Ocean Fe-Mn deposits. *Geochimica et Cosmochimica Acta 65* (23): 4303–4319. https://doi.org/10.1016/S0016-7037(01)00713-X

Vu, T.D.H. and Sohrin, Y. (2013). Diverse stoichiometry of dissolved trace metals in the Indian Ocean. *Scientific Reports 3*: 1745. https://doi.org/10.1038/srep01745

Wang, H., Yang, Q., Ji, F. et al. (2012). The geochemical characteristics and Fe (II) oxidation kinetics of hydrothermal plumes at the Southwest Indian Ridge. *Marine Chemistry 134–135*: 29–35. https://doi.org/10.1016/j.marchem.2012.02.009

Wang, L., Cheung, M.K., Kwan, H.S. et al. (2015). Microbial diversity in shallow-water hydrothermal sediments of Kueishan Island, Taiwan as revealed by pyrosequencing. *Journal of Basic Microbiology 55* (11): 1308–1318. https://doi.org/10.1002/jobm.201400811

Wang, Y., Han, X., Petersen, S. et al. (2017). Mineralogy and trace element geochemistry of sulfide minerals from the Wocan Hydrothermal Field on the slow-spreading Carlsberg Ridge, Indian Ocean. *Ore Geology Reviews 84*, 1–19. https://doi.org/10.1016/j.oregeorev.2016.12.020

Wartiainen, I., Hestnes, A.G., McDonald, I.R. et al. (2006). Methylobacter tundripaludum sp. nov., a methane-oxidizing bacterium from Arctic wetland soil on the Svalbard islands, Norway (78°N). *International Journal of Systematic and Evolutionary Microbiology 56* (1): 109–113. https://doi.org/10.1099/ijs.0.63728-0

Watanabe, H. and Beedessee, G. (2015). Vent fauna on the central Indian ridge. In: *Subseafloor Biosphere Linked to Hydrothermal Systems: TAIGA Concept* (eds. J. Ishibashi, K. Okino and M. Sunamura), 205–212. Springer. https://doi.org/10.1007/978-4-431-54865-2_16

Watanabe, H., Fujikura, K., Kojima, S. et al. (2010). Japan: vents and seeps in close proximity. In: Topics in Geobiology (eds. N.H. Landman and P. Harries), 379–401. https://doi.org/10.1007/978-90-481-9572-5_12

Watanabe, H.K., Chen, C., Marie, D.P. et al. (2018). Phylogeography of hydrothermal vent stalked barnacles: a new species fills a gap in the Indian Ocean ‘dispersal corridor’ hypothesis. *Royal Society Open Science 5* (4). https://doi.org/10.1098/rsos.172408

Wilson, D.J., Piotrowski, A.M., Galy, A. et al. (2012). A boundary exchange influence on deglacial neodymium isotope records from the deep western Indian Ocean. *Earth and Planetary Science Letters 341–344*: 35–47. https://doi.org/10.1016/j.epsl.2012.06.009

Winn C.D., Karl D.M. and Massoth G.J. (1986). Microorganisms in deep-sea hydrothermal plumes. *Nature 320*: 744–746.

Winn, C.D., Cowen, J.P. and Karl, D.M. (1995). Microbes in deep-sea hydrothermal plumes. In: *The Microbiology of Deep-Sea Hydrothermal Vents* (ed. D. Karl), 255–273. Boca Raton, FL: CRC Press.

Winn, C.D., Karl, D.M. and Massoth, G.J. (1986). Microorganisms in deep-sea hydrothermal plumes. *Nature 320* (6064): 744–746. https://doi.org/10.1038/320744a0

Wu, Y., Cao, Y., Wang, C. et al. (2014). Microbial community structure and nitrogenase gene diversity of sediment from a deep-sea hydrothermal vent field on the Southwest Indian Ridge. *Acta Oceanologica Sinica 33* (10): 94–104. https://doi.org/10.1007/s13131-014-0544-0

Yang, W., Tao, C., Li, H. et al. (2017). 230 Th/238 U dating of hydrothermal sulfides from Duanqiao hydrothermal field, Southwest Indian Ridge. *Marine Geophysical Research 38* (1–2): 71–83.

Yu, Z., Li, H., Li, M. et al. (2018). Hydrothermal signature in the axial-sediments from the Carlsberg Ridge in the northwest Indian Ocean. *Journal of Marine Systems 180*: 173–181. https://doi.org/10.1016/j.jmarsys.2016.11.013

Yu, J., Tao, C., Liao, S. et al. (2021). Resource estimation of the sulfide-rich deposits of the Yuhuang-1 hydrothermal field on the ultraslow-spreading Southwest Indian Ridge. *Ore Geology Reviews 134*: 104169.

Yuan, J., Lai, Q., Sun, F. et al. (2015). The diversity of PAH-degrading bacteria in a deep-sea water column above the southwest Indian ridge. *Frontiers in Microbiology 6*. https://doi.org/10.3389/fmicb.2015.00853

Yue, X., Li, H., Ren, J. et al. (2019). Seafloor hydrothermal activity along mid-ocean ridge with strong melt supply: study from segment 27, southwest Indian ridge. *Scientific Reports*, *9* (1). https://doi.org/10.1038/s41598-019-46299-1

Zhang, L., Kang, M., Xu, J. et al. (2016). Bacterial and archaeal communities in the deep-sea sediments of inactive hydrothermal vents in the Southwest India Ridge. *Scientific Reports 6*. https://doi.org/10.1038/srep25982

Zhang, B., Li, Z., Hou, Z. et al. (2018). Mineralogy and Chemistry of Sulfides from the Longqi and Duanqiao Hydrothermal Fields in the Southwest Indian Ridge. *Acta Geologica Sinica-English Edition 92* (5): 1798–1822.

Zhou, Y., Zhang, D., Zhang, R. et al. (2018). Characterization of vent fauna at three hydrothermal vent fields on the Southwest Indian Ridge: Implications for biogeography and interannual dynamics on ultraslow-spreading ridges. *Deep-Sea Research Part I: Oceanographic Research Papers 137*: 1–12. https://doi.org/10.1016/j.dsr.2018.05.001